

Response to Reviewers – August 2020

Reviewer #1

The authors have done a good job in addressing my comments. I recommend the paper be accepted.

Many thanks for this. We have made changes in response to your comments below in addition to adding the URL for the CEDA archive link to the dataset where it will be given a DOI.

Two minor comments:

- fig 5: It is a good idea to change the color of the noQC boxes to grey, but they still look blue to me!

Many apologies for not getting this right the first time – and my spelling error of gray! I have now changed the 'no QC' boxes to grey and amended the figure caption to reflect this.

- The companion dataset HadISDH land uses a statistical approach (pairwise homogenization) to find change points and adjust for non-climatic changes. Presumably this can't be done for ships because there are not fixed neighbors. It would be helpful to add a couple of sentences to discuss the absence of this kind of statistical homogenization for marine datasets and what it means for the robustness of trends in the land and marine versions of the dataset.

This is a good point. Actually, we struggled to leave it at just a couple of sentences so have added a rather large paragraph at the beginning of the section on bias adjustment (3.3):

"The availability of machine readable metadata alongside each observation enables specific adjustment for known biases and inhomogeneities. This differs to the approach for the HadISDH.land dataset where no substantial digitised metadata currently exists. By necessity, adjustment for biases (inhomogeneities) is done using the Pairwise Homogenisation Algorithm (Menne and Williams, 2009). This is a neighbour comparison based statistical algorithm to detect change points and resolve the most reasonable adjustments. It is very likely that inhomogeneities that affect the land data such as instrument changes, instrument housing changes and practice changes also affect the marine data. However, this level of detail is not available in the metadata, nor is it straightforward to adjust for even if it was because of the mobile nature of ship data. Although a neighbour based comparison is possible and useful at the single observation level (e.g. buddy check), it is not useful in the manner in which it is used for land observations from static weather stations. Arguably, the region-wide biases such as increasing ship heights and ventilation biases are of greater concern for long term trends than the more ship specific inhomogeneity owing to instrument or housing changes. We acknowledge that, similar to the land data, there will be inhomogeneity/bias remaining within the HadISDH.marine dataset which we cannot detect or adjust for but argue that we have removed the large errors from the dataset. Future versions will take advantage of greater metadata and statistical tools as they become available."

Reviewer #2

I have read through the revised paper and understood that authors have addressed the points raised by reviewers appropriately.
Before acceptance, the following technical corrections are suggested.

Many thanks for your second review. We have made changes in response to your comments below in addition to adding the URL for the CEDA archive link to the dataset where it will be given a DOI.

L237: Put "." after "residual uncertainty".

DONE

L791: Insert space for "havebecome".

DONE

Figure 1 (caption): To refer to the JRA-55 reanalysis product, it would be appropriate to cite Kobayashi et al. (2015) instead of Ebita et al. (2011).

###

Kobayashi, S., Ota, Y., Harada, Y., Ebita, A., Moriya, M., Onoda, H., Onogi, K., Kamahori, H., Kobayashi, C., Endo, H., Miyaoka, K., and Takahashi, K.: The JRA-55 reanalysis: general specifications and basic characteristics, J. Meteor. Soc. Japan, 93, 5–48, <https://doi.org/10.2151/jmsj.2015-001>, 2015.

###

DONE

Figure 12 (caption): Replace "." with "," after (Santer et al. 2008).

DONE

1 **Development of the HadISDH marine humidity climate monitoring dataset**

2 Kate M. Willett¹, Robert J. H. Dunn¹, John J. Kennedy¹ and David I. Berry²

3

4 ¹Met Office Hadley Centre, Exeter, UK

5 ²National Oceanography Centre, Southampton, UK

6

7 *Correspondence to:* Kate Willett kate.willett@metoffice.gov.uk

8

9 **Abstract**

10

11 Atmospheric humidity plays an important role in climate analyses. Here we describe the production and key
12 characteristics of a new quasi-global marine humidity product intended for climate monitoring,
13 HadISDH.marine. It is an in-situ based multi-variable marine humidity product, gridded monthly at a 5° by 5°
14 spatial resolution from January 1973 to December 2018 with annual updates planned. Currently, only reanalyses
15 provide up to date estimates of marine surface humidity but there are concerns over their long-term stability. As
16 a result, this new product makes a valuable addition to the climate record and will help address some of the
17 uncertainties around recent changes (e.g. contrasting land and sea trends, relative humidity drying). Efforts have
18 been made to quality control the data, ensure spatial and temporal homogeneity as far as possible, adjust for
19 known biases in non-aspirated instruments and ship heights, and also estimate uncertainty in the data.
20 Uncertainty estimates for whole-number reporting and for other measurement errors have not been quantified
21 before for marine humidity. This is a companion product to HadISDH.land, which, when combined will provide
22 methodologically consistent land and marine estimates of surface humidity.

23

24 The spatial coverage of HadISDH.marine is good over the Northern Hemisphere outside of the high latitudes but
25 poor over the Southern Hemisphere, especially south of 20° S. The trends and variability shown are in line with
26 overall signals of increasing moisture and warmth over oceans from theoretical expectations and other products.
27 Uncertainty in the global average is larger over periods where digital ship metadata are fewer or unavailable but
28 not large enough to cast doubt over trends in specific humidity or air temperature. Hence, we conclude that
29 HadISDH.marine is a useful contribution to our understanding of climate change. However, we note that our

30 ability to monitor surface humidity with any degree of confidence depends on the continued availability of ship
31 data and provision of digitised metadata.

32

33 HadISDH.marine data, derived diagnostics and plots are available at

34 www.metoffice.gov.uk/hadobs/hadisdh/indexMARINE.html and

35 <http://dx.doi.org/10.5285/463b2fcd6a264a39b1e3249dab16c177> (Willett et al., 2020).

36

37 **1 Introduction**

38

39 Water vapour plays a key role as a greenhouse gas, in the dynamical development of weather systems, and
40 impacts society through precipitation and heat stress. Over land, all these aspects are important and recent
41 changes have been assessed by Willett et al. (2014). Over the oceans, a major source of moisture over land, a
42 similar analysis is essential to enhance our understanding of the observed changes generally and as a basis for
43 worldwide evaluation of climate models. In recognition of its importance, the surface atmospheric humidity has
44 been recognised as one of the Global Climate Observing System (GCOS) Essential Climate Variables (ECVs)
45 (Bojinski et al., 2014; <https://gcos.wmo.int/en/essential-climate-variables>).

46

47 Observational sources of humidity over the ocean are limited. The NOCSv2.0 (Berry and Kent, 2011) is the
48 only recently updated (January 1971 to December 2015) marine surface humidity monitoring product based on
49 in-situ observations, but it only includes specific humidity (q). Satellite based humidity products exist (e.g.
50 HOAPS, Fennig et al., 2012) but these rely on the in-situ observations for calibration. Whilst quasi-global, the
51 uncertainties in the NOCSv2.0 product are large outside the northern mid-latitudes. In this region the NOCSv2.0
52 product shows a reasonably steadily rising trend over the period of record, similar to that seen over land but with
53 slightly different year-to-year variability. Most notably, 2010, a peak year over land in specific humidity, does
54 not stand out over ocean. Figure 1 and Willett et al. (2019) show global land and ocean specific humidity and
55 relative humidity (RH) series from available in-situ and reanalyses products. Older, static products for the
56 ocean (HadCRUH – Met Office **H**adley Centre and **C**limatic **R**esearch **U**nit **H**umidity dataset: Willett et al.,
57 2008; Dai: Dai 2006) show increasing specific humidity to 2003 with similar variability to NOCSv2.0, and near-
58 constant relative humidity. Both HadCRUH and Dai show a positive relative humidity bias pre-1982 and
59 slightly higher specific humidity over 1978-1984 compared to NOCSv2.0. There is broad similarity between the

60 reanalysis products and the in-situ products but with notable differences for specific humidity in the scale of the
61 1998 peak and the overall trend magnitude. Differences are to be expected given that the reanalyses are spatially
62 complete in coverage, albeit derived only from their underlying dynamical models over data sparse regions. The
63 reanalyses exhibit near-constant to decreasing relative humidity over oceans but with poorer agreement between
64 both the reanalyses themselves and compared to the in-situ products over land. This is to be expected given the
65 larger sources of bias and error over ocean (Sect. 2) and sparse data coverage. Importantly, land and marine
66 specific humidity appear broadly similar whereas for relative humidity, the distinct drying since 2000 over land
67 is not apparent over ocean in reanalyses and the previously available in-situ products finish too early to be
68 informative. Note that the HadISDH.marine described herein is shown here for comparison and will be
69 discussed below.

70

71 A positive bias in global marine average relative humidity pre-1982 is apparent in Dai and HadCRUH, and has
72 previously been attributed to high frequencies of whole numbers in the dew point temperature observations prior
73 to January 1982 (Willett et al., 2008). This is less clear in the global average specific humidity timeseries.

74 ICOADS (International Comprehensive Ocean-Atmosphere Dataset) documentation

75 (<http://icoads.noaa.gov/corrections.html>) notes issues with the pre-1982 data especially mixed-precision

76 observations, where the air temperature has been recorded to decimal precision but the dew point temperature is
77 only available as a whole number. Such reporting was in accordance with the WMO Ship Code before 1982.

78 The documentation notes a truncation error in the dew point depression which would lead to a positive bias in
79 relative humidity. Alternatively, Berry (2009) show that patterns in the North Atlantic Oscillation coincide with
80 this time period and could have played a role. The NOCSv2.0 product is based on reported wet bulb temperature
81 rather than dew point temperature, where decimal precision is usually present. Hence, the NOCSv2.0 product is
82 expected to be unaffected by these rounding issues. Our analysis shows that changes to the code in January 1982
83 did not eliminate whole number reporting and high frequencies of whole numbers can be found throughout the
84 record in both air temperature and dew point temperature (Sect. 2.4 and Sect. 3.4).

85

86 Clearly, there is a need for more and up to date in-situ monitoring of humidity over ocean, especially for RH.

87 The structural uncertainty in estimates can only be explored if there are multiple available estimates so a new
88 product that explores different methodological choices, and extends the record, is complementary to the existing
89 NOCSv2.0 product and reanalyses estimates. Here we report the development of a multi-variable marine

90 humidity analysis HadISDH.marine.1.0.0.2018f (Willett et al., 2020). HadISDH.marine is a Met Office **Hadley**
91 Centre led **I**ntegrated **S**urface **D**ataset of **H**umidity, forming a companion product to the HadISDH.land
92 monitoring product, and enabling the production of a blended global land and ocean product. We use existing
93 methods where possible from the systems used for building the long running HadSST dataset (Kennedy et al.,
94 2011a, 2011b, 2019), and also use some of the bias adjustment methods employed for NOCSv2.0 (Berry and
95 Kent 2011). We have explored the data to design new humidity specific processes where appropriate,
96 particularly in terms of quality control and gridding.

97
98 HadISDH.marine is a climate-quality 5° by 5° gridded monthly mean product from 1973 to present (December
99 2018 at time of writing) with annual updates envisaged. Fields will be presented for surface (~10 m) specific
100 humidity, relative humidity, vapour pressure, dew point temperature, wet bulb temperature and dew point
101 depression. Air temperature will also be made available as a by-product but less attention has been given to
102 addressing temperature specific biases. The product is intended for investigating long-term changes over large
103 scales and so efforts have been made to quality control the data, ensure spatial and temporal homogeneity, adjust
104 for known biases and also estimate remaining uncertainty in the data. In particular, we estimate uncertainties
105 from whole-number reporting and other measurement errors that have not been quantified before for marine
106 humidity.

107
108 Section 2 discusses known issues with marine humidity data. Section 3 describes the source data and all
109 processing steps. Section 4 presents the gridded product and explores the different methodological choices and
110 comparison with NOCSv2.0 specific humidity and ERA-Interim marine humidity. This section also includes a
111 first look at the blended land and marine HadISDH product for each variable. Section 5 covers data availability
112 and Section 6 concludes with a discussion of the strengths and weaknesses of the product.

113

114 **2 Known issues affecting the marine humidity data**

115

116 **2.1 Daytime solar-biases**

117

118 Marine air temperature measurements on board ships during the daytime are known to be affected by the heating
119 of the ship or platform by the sun. This results in a positive bias during daylight and early night time hours. The

120 bias varies with sunlight strength/cloudiness (and thus also latitude), relative wind speed, size and material of
121 the ship. This solar heating bias affects both the wet bulb and dry bulb temperature measurements but, as noted
122 by Kent and Taylor (1996), the ships do not act as a source of humidity or change the humidity content of the
123 air. As a result, biases in the specific humidity and dew point temperature due to the solar heating errors will be
124 negligible. However, care needs to be taken with relative humidity because estimates of the saturation vapour
125 pressure from the uncorrected dry bulb air temperature will be too high, leading to an underestimate in relative
126 humidity. Ideally, relative humidity should be estimated using the corrected dry-bulb temperature to calculate
127 the saturation vapour pressure and uncorrected wet and dry bulb temperature or dew point temperature to
128 calculate the vapour pressure.

129

130 Previously, efforts have been made to bias-adjust the air temperature observations for solar heating by
131 modelling the extra heating over the superstructure of the ship, taking account of the relative wind speed,
132 cloudiness, time of day, time of year and latitude (Kent et al, 1993; Berry et al., 2004; Berry and Kent, 2011).
133 These adjustments are complex and so we have decided not to attempt to implement them for our first version of
134 a marine humidity product given the wide variety of other issues we have accounted for. We have, however,
135 produced daytime, night time and combined products to investigate differences that may be caused by the solar
136 heating bias. Later versions of HadISDH.marine that apply bias corrections for solar heating may reduce the
137 amount of daytime data removed.

138

139 **2.2 Un-aspirated psychrometer bias**

140

141 Humidity measurements can be made in a variety of ways. Instruments can be housed in a screen with
142 ventilation slats, with or without additional artificial aspiration, or handheld in a sling or whirling psychrometer.
143 There is information on instrument ventilation provided up to 2014. Approximately 30 % of ship observations
144 have information in 1973, peaking at ~75 % by the mid-1990s, as summarised in Fig. 2. Initially, slings were
145 more common for the hygrometer and thermometer, but by 1982 a screen was more common. There is a
146 tendency for the screened instruments, in the absence of artificial aspiration, to give a wet bulb reading that is
147 higher relative to the slings/whirling instruments where airflow is ensured by the whirling motion. Bias
148 adjustments have been applied to un-aspirated humidity observations by Berry and Kent (2011), building on
149 previous bias adjustments of Josey et al. (1999) and Kent et al. (1993). They have also estimated the uncertainty

150 in the bias adjustments. We implement a modified version of their method of bias adjustment for the un-
151 aspirated observation types (Sect. 3.3.1) and uncertainty estimation. Uncertainties from instrument bias
152 adjustments will have some spatial and temporal correlation structure as the ships move around (Kennedy et al.,
153 2011a).

154

155 **2.3 Ship height inhomogeneity**

156

157 Over time there has been a general trend for ship heights to increase. Kent et al. (2007; 2013) quantified the
158 increase from an average of ~ 16m in 1973 to ~24m by the end of 2006. Instrument height information is
159 available for some ships between the period of 1973 and 2014, providing heights for the barometer (HOB),
160 thermometer (HOT), anemometer (HOA) and visual observing platform (HOP). Figure 3 shows the availability
161 of height information and the mean and standard deviation of heights per year in each category for the ship
162 observations selected here. Similar to the ventilation metadata, height information availability is low in 1973,
163 peaking mid-1990s to 2000 and then declining slightly. Prior to 1994 only the platform height was available
164 from WMO Publication 47. This was replaced in 1994 by the barometer height and augmented with the
165 thermometer and visual observing heights from 2002 onwards (Kent et al., 2007). Anemometer heights have
166 been available from WMO 47 since 1970. All four types of heights increase over time. We conclude that the
167 mean height based on HOP/HOB/HOT increases from 17 m in 1973 to 23 m by 2014, which differs slightly to
168 that in Kent et al., (2007). If uncorrected, this likely leads to a small artificial decreasing trend in air temperature
169 and specific humidity, as, in general, these variables decrease with height away from the surface. The effect on
170 relative humidity is less clear and depends on the relative effects on air temperature and specific humidity.

171

172 Prior studies (e.g. Berry and Kent, 2011; Berry 2009; Josey et al., 1999; Rayner et al., 2003; Kent et al., 2013)
173 have applied height adjustments to the air temperature, specific humidity and wind speed measurements to
174 adjust the measurements to a common reference height and minimise the impact of the changing observing
175 heights on the climate record. These have been based on boundary layer theory and the bulk formulae, using the
176 parameterisations of Smith (1980, 1988). In the absence of high-frequency observations of meteorological
177 parameters for each observation location, allowing direct estimation of the surface fluxes, parameterisations
178 have to be made and an iterative approach is necessary to estimate a height adjustment (Sect. 3.3.2). We have
179 followed these previous approaches and estimated height adjustments for all observations and variables of

180 interest. Where observing heights are unavailable we have made new estimates (Sect. 3.3.2). We have also
181 provided an estimate of uncertainty on these height adjustments, which are larger where we have also estimated
182 the height of the observation. The uncertainties from height adjustments will have some spatial and temporal
183 correlation structure.

184

185 **2.4 Whole-number reporting biases**

186

187 Recording and reporting formats and practices have changed many times over the 20th century, affecting the
188 climate record. Some formats required the wet bulb temperature to be reported, others the dew point temperature
189 and some allowed either or both ([https://www.wmo.int/pages/prog/amp/mmop/documents/publications-](https://www.wmo.int/pages/prog/amp/mmop/documents/publications-history/history/SHIP.html)
190 [history/history/SHIP.html](https://www.wmo.int/pages/prog/amp/mmop/documents/publications-history/history/SHIP.html)). Some earlier formats restricted space to reporting temperature to whole numbers
191 only and this practice has continued with some ships continuing to report the dew point (or wet bulb)
192 temperature and sometimes even the dry bulb temperature to whole numbers. A practice of truncation of the
193 dew point depression has been noted for the pre-1982 data (<http://icoads.noaa.gov/corrections.html>) which
194 would result in spuriously high humidity (both in relative and actual terms). It is clear from the
195 ICOADS3.0.0/3.0.1 data that there has been a practice of reporting values to whole numbers rather than decimal
196 places, both for air temperature and dew point temperature. Rounding dew point temperature and air
197 temperature could result in a +/- 0.5° C error individually or a just less than +/- 1° C error in dew point
198 depression for a worst-case scenario combination.

199

200 Whole-number reporting is an issue throughout the record for both variables – a breakdown of air and dew point
201 temperature by decimal place over time is shown in Fig. S1. Air temperature also shows a disproportionate
202 frequency of half degrees (5s). The percentage of whole numbers (0s) declines over time, dramatically in the
203 mid- to late 1990s for air temperature and from 2008 for both air and dew point temperature. This decline in the
204 1990s, and in part also the general decline, appears to be linked to an increase in numbers of moored buoys (see
205 Fig. 5), a similar analysis without the moored buoys (not shown) shows greater consistency over time. The dew
206 point temperature has two distinct peaks in whole number frequency in the 1970s and mid-1990 to early 2010s.
207 The latter peak is more pronounced when moored buoys are not included. The early peak is somewhat
208 consistent with the restriction in transmission space prior to January 1982. This was previously thought to have
209 been a possible cause of higher relative humidity over the period 1973-1981 compared to the rest of the record

210 in the HadCRUH marine relative humidity product (Willett et al., 2008). The pre-1982 moist bias was also
211 apparent in the global marine relative humidity product of Dai (2006), which like HadCRUH used dew point
212 temperatures. The NOCSv2.0 product preferentially utilises the wet bulb temperatures from ICOADS which are
213 not affected by whole number reporting to the same extent.

214

215 Rounding of temperature alone should not affect the mean dew point temperature, specific humidity or vapour
216 pressure. However, as with the solar bias issue, it is sensitive to at what point the reported dew point
217 temperature was derived from the measured wet bulb temperature or relative humidity. Most likely, this would
218 be done prior to any rounding or truncating for reporting but during later conversion of various sources into
219 digital archives, or corrections, the dew point temperature may have been reconstructed
220 (https://icoads.noaa.gov/e-doc/other/dupelim_1980). The effect of rounding on a monthly mean gridbox average
221 should be small as these errors are random and should reduce with averaging. However, there is a risk of
222 removing very high humidity observations when a rounded dew point temperature then exceeds a non-rounded
223 air temperature. Such values are removed by our supersaturation check (Sect. 3.2). We do not feel able to
224 correct for this issue but instead include an uncertainty estimate for it. Overly frequent whole numbers are
225 identified both during quality control track analysis and deck analysis. This will be discussed in more detail in
226 Sect. 3.4. Clearly, there are various issues that can arise linked to the precision of measured and reported data in
227 addition to conversion between different units (e.g., Fahrenheit, Celsius and Kelvin, Fig. S1) and between
228 different variables.

229

230 **2.5 Measurement errors**

231

232 All observations are subject to some level of measurement error and, outside of precision laboratory
233 experiments, the errors can be significant. The BIPM Guide to the Expression of Uncertainty in Measurement
234 (BIPM, 2008) describes two categories of measurement uncertainty evaluation. A Type A evaluation estimates
235 the uncertainty from repeated observations. A Type B evaluation of the uncertainty is based on prior knowledge
236 of the instrument and observing conditions. Within this study we use a Type B evaluation, adjusting for
237 systematic errors and inhomogeneities due to inadequate ventilation and changing observing heights (screen and
238 height adjustments) and estimate the residual uncertainty. For the random components, we make the
239 conservative assumption that all measurements were taken using a psychrometer (wet bulb and dry bulb

240 thermometers), which allows us to follow the HadISDH.land methodology of Willett et al. (2013, 2014) as
241 described in Sect. 3.4. An assessment of the frequency of hygrometer types (TOH) within our selected
242 ICOADS3.0.0/3.0.1 data shows this to be a fair assumption as the vast majority of ships (where metadata is
243 available: ~30 % increasing to ~70 % 1973 to 1995 then decreasing to 60 % by 2014) are listed as being from a
244 psychrometer (Fig. 4). Electric sensors are becoming more common and made up ~30 % of observations by
245 2014 (the end of the metadata information). There are no instrument type metadata for ocean platforms or
246 moored buoys. As it is likely that most buoy observations are made using RH sensors, we plan to develop an RH
247 sensor specific measurement uncertainty in future versions.

248

249 **2.6 Other sources of error**

250

251 There are other issues specific to humidity measurements that may be further sources of error. Hygrometers that
252 require a wetted wick (i.e., psychrometers), and thus a source of water, are vulnerable to the wick drying out or
253 contamination, especially by salt in the marine environment. The wick drying results in erroneous relative
254 humidity readings of 100 %rh where the wet bulb essentially behaves identically to the dry bulb thermometer.
255 There can also be issues when the air temperature is close to freezing depending on whether the wet bulb has
256 become an ice bulb or not and whether wet bulb or ice bulb calculations are used in any conversions. Humidity
257 observing in low temperature can be generally problematic. For radiosondes, there has previously been a
258 practice of recording a set low value when the humidity observation falls below a certain value (Wade 1994,
259 Elliott et al. 1998). It is debateable how likely such low humidity values are over oceans and this practice has
260 not been documented for ship observations. However, the set value issue is something to look out for. Wet bulb
261 thermometers (and other instruments) can experience some hysteresis at high humidity where it takes some time
262 to return to a lower reading. The wet bulb also requires adequate ventilation which has been discussed above.

263

264 These can be accounted for to a large extent through quality control but some error will inevitably remain. We
265 can increase our confidence in the data by comparison with other available products and general expectation
266 from theory.

267

268 **3 Construction of the gridded dataset and uncertainty estimates**

269

270 ICOADS Release 3.0 (Freeman et al., 2017) forms the base dataset for the HadISDH.marine humidity products.
271 From January 1973 to December 2014 we use ICOADS.3.0.0 from <http://rda.ucar.edu/datasets/ds540.0/>. These
272 data include a unique identifier (UID) for each observation, a station identifier/ship callsign (ID), metadata on
273 instrument type, exposure and height in many cases. From January 2015 onwards we use ICOADS.3.0.1 from
274 the same source. These data include an ID and UID but no instrument metadata. It is likely that digitised
275 metadata updates will be available periodically, depending on resource availability. Each observation is
276 associated with a deck number. These are identifiers for ICOADS national and trans-national sub-sets of data
277 relating to source e.g., deck 926 is the International Maritime Meteorological (IMM) data
278 (<https://icoads.noaa.gov/translation.html>). We utilise the reported air temperature (T) and reported dew point
279 temperature (T_d) as the source for our humidity products. Sea surface temperature (SST) and wind speed (u) are
280 used for estimating height adjustments.

281

282 We calculate the specific humidity (q), relative humidity (RH), vapour pressure (e), wet bulb temperature (T_w ,
283 not the thermodynamic wet bulb but a close approximation to it) and dew point depression (DPD) for each point
284 observation. All humidity variables are derived from reported air and dew point temperature and ERA-Interim
285 climatological (from the nearest 1° by 1° 5 day mean [pentad] gridbox) surface pressure P_s , using the set of
286 equations from Willett et al., (2014) which can be found in Table S1. This provides consistency with
287 HadISDH.land for later merging. For consistency we use a fixed psychrometric coefficient that is identical for
288 all observations when estimating the approximate thermodynamic wet bulb temperature rather the observed
289 value which depends on the type of psychrometer used. This is also consistent with what is done for
290 HadISDH.land.

291

292 Additionally, we use ERA-Interim (Dee et al., 2011) reanalysis data to provide initial marine climatologies and
293 climatological standard deviations for all variables to complete a 1st iteration climatological outlier test. We
294 extract 1° by 1° gridded 6 hourly 2 m air and dew point temperature and surface pressure to create 6 hourly
295 humidity variables and then pentad climatologies and standard deviations over the 1981-2010 period. Note that
296 3 iterations are passed before finalising the product. Only the 1st iteration uses ERA-Interim climatologies, later
297 iterations use climatologies built from the previous iteration's quality-controlled observations (Sects. 3.2, 3.5,
298 4.1).

299

300 The construction process, including the three iterations and all outputs, is visualised in Figure 5. Firstly,
301 humidity variables are calculated. For the 1st iteration the hourly temperature and dew point temperature data are
302 quality controlled (section 3.1) using an ERA-Interim based climatology. The data are then gridded, merged and
303 a 1° by 1° pentad climatology produced for each variable (section 3.5). These 1st iteration climatologies are then
304 used to quality control the original hourly data again; these data are then gridded, merged and a 2nd iteration
305 climatology produced. The 2nd iteration climatology is then used to quality control the original hourly data for a
306 third and final time. It is during this 3rd iteration that bias adjustments are applied and uncertainties estimated.
307 The bias adjusted data and uncertainties are then gridded, merged and climatologies created. For future annual
308 updates the 2nd iteration climatologies will be used to apply quality control. Having three iterations enables
309 incremental improvements to the climatology used to quality control the data and therefore the skill of the
310 quality control tests. It means that we can ensure that no artefacts remain from using ERA-Interim to quality
311 control the data initially. Arguably more iterations could be done but each one is computationally expensive and
312 the difference between the 2nd and 3rd iteration is already very small.

313

314 **3.1 Data selection**

315

316 We screen all ICOADS data to sub-select only those observations passing the following criteria:

- 317 - there must be a non-missing T and T_d value;
- 318 - the platform type (PT) must be in one of the following categories: a ship (a US Navy or unknown
319 vessel, a merchant ship or foreign military ship, an ocean station vessel off station /at an unknown
320 location, an ocean station vessel on station, a lightship, an unspecified ship - PT = 0, 1, 2, 3, 4, 5);
321 or a stationary buoy (moored or ice buoy - PT = 6, 8);
- 322 - the observation must have a climatology and standard deviation available for its closest 1° by 1°
323 pentad;
- 324 - the observation must pass the gross error checks: calculated RH must be between 0 and 150 %rh
325 (supersaturated values are flagged during quality control); both T and T_d must be between -80 and
326 65 °C; and calculated q must be greater than 0.0 g kg⁻¹;
- 327 - latitudes must be between -90° and 90° and longitudes must be between -180° and 360° (later
328 converted to -180° to 180°);
- 329 - the hour, day, month and year must be valid quantities;

330 any observation from Deck 732 from a specified year and region is blacklisted (Rayner et al., 2006, Kennedy et
331 al, 2011a, Table S2).

332

333 Other marine products (e.g., NOCSv2.0; Berry and Kent, 2011) solely use ship observations due to the lack of
334 buoy metadata available. We include moored buoys to produce climatologies because spatial coverage is of high
335 importance. Our final version recommended to users is a ship-only (SHIP) product but we have produced a
336 combined (ALL) product for comparison. This will be reassessed for future versions. Figure 6a shows the
337 number of observations included in the initial selection per year, broken down by platform type. The breakdown
338 for day and night time observations individually is near identical (not shown). Ship (PT = 5) observations make
339 up almost the entire dataset until the 1990s. After this the number of moored buoys grows significantly to make
340 up around ~50 % of observations from 2000 onwards. The ship-only product (removal of moored buoys)
341 significantly reduces the number of observations in the recent period but gives a more consistent number of
342 observations throughout the record. Our use of climate anomalies should mitigate biasing due to uneven
343 sampling to some extent. Note that the number of gridboxes containing data may be a more relevant measure
344 and that the vast increase in the number of buoys has not actually resulted in the same level of increase in spatial
345 coverage in terms of gridboxes (compare 2018 annual average maps for ship-only and combined
346 HadISDH.marine in Fig. S2).

347

348 **3.2 Quality control processing**

349

350 We have not used any of the pre-set flags from ICOADS processing to ensure methodological independence of
351 HadISDH and a process that allows for exploration and analysis of different methodological choices. The
352 quality control processing employed here largely follows the methodology for HadSST4 (Kennedy et al., 2019)
353 with some changes to the climatology check and buddy check thresholds to increase regional sensitivity and
354 additional humidity specific checks. A flag for whole number prevalence has also been added but this is used for
355 uncertainty estimation and not to remove an observation. All observations have their nearest 1° by 1° pentad
356 mean climatology (source depends on iteration – Sect. 3.5) subtracted to create a climate anomaly.

357

358 Each observation is passed through a suite of quality control tests which are summarised in Table 1 along with
359 whether the quality control tests are used to remove or just to flag the observations, and the stage of processing

360 at which they are applied. The climatology check differs from the static HadSST3 threshold of climatology for
361 air temperature of +/- 8° C. We have allowed for a variable threshold depending on the nearest 1° by 1° pentad
362 climatology standard deviation σ . This is set at 5.5 σ . It accounts for the lower variability in the tropics and
363 greater variability in the mid-latitudes. We have set minimum and maximum σ values of 1° C and 4° C
364 respectively resulting in a minimum range of +/- 5.5° C and a maximum range of +/- 22° C. Several thresholds
365 were tested with the selected threshold balancing avoiding acute cut-offs in the data distribution while still
366 removing obviously bad data (Figs. S3 to S6). Given that outliers are assessed by comparing a point observation
367 with a 1° by 1° pentad mean the thresholds have to be relatively large.

368

369 The buddy check compares each observation's climate anomaly with the average of the climate anomalies of its
370 nearest neighbours in space and time, expanding the search area in space and time as necessary until at least one
371 neighbour observation is found. The permitted difference is set by the climatological standard deviation of the
372 candidate 1° by 1° pentad gridbox multiplied by an amount dependent on the number of neighbours present.

373 There are five levels of searches:

- 374 1. $\pm 1^\circ$ latitude and longitude and ± 2 pentads: the climatological standard deviation is multiplied by
375 5.5, 5.0, 4.5 and 4.0 for 1-5, 6-15, 16-100 and >100 neighbouring observations respectively;
- 376 2. $\pm 2^\circ$ latitude and longitude and ± 2 pentads: the climatological standard deviation is multiplied by
377 5.5 for >1 neighbouring observation;
- 378 3. $\pm 1^\circ$ latitude and longitude and ± 4 pentads: the climatological standard deviation is multiplied by
379 5.5, 5.0, 4.5 and 4.0 for 1-5, 6-15, 16-100 and >100 neighbouring observations respectively;
- 380 4. $\pm 2^\circ$ latitude and longitude and ± 4 pentads: the climatological standard deviation is multiplied by
381 5.5 for >1 neighbouring observation;
- 382 5. no neighbour $\pm 2^\circ$ latitude and longitude and ± 4 pentads: the threshold is set at 500.

383 The thresholds used for the buddy check are wider than those previously used in HadSST3. This is to account
384 for the greater variability of air and dew point temperature, and sparser observation coverage. It is only applied
385 in the 3rd iteration of the quality control (Sect. 3.5).

386

387 Figure 6 shows the final number of observations passing through initial selection and then 3rd iteration quality
388 control by platform (PT) type. The quality control does not significantly affect one platform over another. The
389 performance of these tests is demonstrated for 4 example months in Figs. S3 to S6. These reveal a slight positive

390 bias in the removed air temperature observations and negative bias in removed dew point temperature.
391 Removals in terms of relative humidity and specific humidity similarly tend to have a negative bias. It is clear
392 that the majority of grossly erroneous observations are removed. The change in climatology between iterations
393 of the quality control process (Sect. 3.5) also makes a difference to removals. This is both because the
394 observation driven climatologies do not provide complete spatial coverage and because the ERA-Interim
395 climatologies are cooler and drier than the observations (Sect. 4.1). Removals are dense in the Northern
396 Hemisphere and especially sparse around the tropics. The addition of the buddy check in the 3rd iteration
397 considerably increases the removal rate, noticeably over the Southern Hemisphere and Tropics.

398

399 The quality-control flagging rate for the 3rd iteration reduces over time from ~25 % to ~18 %, as shown in Fig.
400 S7. This is driven by the buddy check and track check. Proportionally more observations are flagged during the
401 daytime than night time but the interannual behaviour is very similar. The daytime increase is driven by the
402 larger number of air temperature buddy and climatology check failures. This could be due to the issue of solar
403 heating of the ship structure during the daytime. The main source of test fails by a large margin is the buddy
404 check, followed by the climatology check and track check. There doesn't appear to be a strong difference in the
405 distribution of removals from each test between the 1973-1981 and 1982-1990 periods that might explain the
406 pre-1982 moist bias (Fig. S8, Sect. 4.2). There is an increase in removals from repeated saturation and
407 supersaturation events over time, particularly the late 2000s. This may be related to the decrease in
408 psychrometer deployment over time and increase in electric and capacitance sensors as shown in Fig. 4. The
409 latter have increased significantly since the mid-2000s.

410

411 The whole number flags show very different behaviour to the other checks and to each other over time in Fig.
412 S7. These depend on the ability to assign each observation to a track/voyage and the frequency of whole number
413 observations on that voyage, hence, these flags are not a true reflection of the whole number frequency.
414 Compared to the actual proportion of whole numbers shown in Fig. S1, these tend to exaggerate the annual
415 patterns but the shape is broadly similar. This method of identifying problematic whole numbers appears to
416 under-sample the true distribution, especially for air temperature pre-1982. An additional deck-based check is
417 applied later for estimating uncertainty from whole numbers (Sect. 3.4).

418

419 Note that the NOCSv2.0 dataset, with which we compare our specific humidity data, includes an outlier check
420 that removes data greater than 4.5 standard deviations from the climatological mean. This test has already been
421 applied within the ICOADS format and so the NOCSv2.0 excludes any data with ICOADS trimming flags set
422 (Wolter 1997). We do not use the trimming flags to select data. They also apply a track check based on Kent and
423 Challenor (2006).

424

425 **3.3 Bias adjustments and associated uncertainties**

426

427 Given the issues raised in Sect. 2, it is desirable to attempt to adjust the observations to improve the spatial and
428 temporal homogeneity and accuracy of the data. As discussed in Sect. 2.1, we have not attempted to adjust for
429 solar biases in this first version product. We have made adjustments for instrument and height biases and
430 estimated uncertainties (summarised in Table 1) in these adjustments.

431

432 The availability of machine readable metadata alongside each observation enables specific adjustment for
433 known biases and inhomogeneities. This differs to the approach for the HadISDH.land dataset where no
434 substantial digitised metadata currently exists. By necessity, adjustment for biases (inhomogeneities) is done
435 using the Pairwise Homogenisation Algorithm (Menne and Williams, 2009). This is a neighbour comparison
436 based statistical algorithm to detect change points and resolve the most reasonable adjustments. It is very likely
437 that inhomogeneities that affect the land data such as instrument changes, instrument housing changes and
438 practice changes also affect the marine data. However, this level of detail is not available in the metadata, nor is
439 it straightforward to adjust for even if it was because of the mobile nature of ship data. Although a neighbour
440 based comparison is possible and useful at the single observation level (e.g. buddy check), it is not useful in the
441 manner in which it is used for land observations from static weather stations. Arguably, the region-wide biases
442 such as increasing ship heights and ventilation biases are of greater concern for long term trends than the more
443 ship specific inhomogeneity owing to instrument or housing changes. We acknowledge that, similar to the land
444 data, there will be inhomogeneity/bias remaining within the HadISDH.marine dataset which we cannot detect or
445 adjust for but argue that we have removed the large errors from the dataset. Future versions will take advantage
446 of greater metadata and statistical tools as they become available.

447

448 **3.3.1 Application of adjustments for biases from un-aspirated instruments**

449

450 We have shown that the majority of humidity observations have been made with a psychrometer (Fig. 4) and
451 that 30-70 % of instruments with metadata available have been housed within a non-aspirated screen (Fig. 2).
452 Berry and Kent (2011) found that applying a 3.4 % reduction to specific humidity observations from non-
453 aspirated screens was a reasonable adjustment to remove the bias relative to aspirated/well ventilated
454 observations (e.g., slings, whirled hygrometers or artificially aspirated instruments). Some uncertainty remains
455 after adjustment which they estimated to be $\sim 0.2 \text{ g kg}^{-1}$. We have used the hygrometer exposure metadata
456 (EOH) or the thermometer exposure (EOT) if EOH does not exist. We assume good ventilation for any
457 instruments that are aspirated (A), from a sling (SL) or ship's sling (SG) or from a whirling instrument (W). We
458 assume poorer ventilation for instruments that are from a screen (S), ship's screen (SN) or are unscreened (US)
459 and apply a bias adjustment. The reported exposure type of Ventilated Screens (VS) does not appear to mean
460 that the screen is artificially ventilated and so bias adjustments are also applied to these. We do not apply
461 adjustments to buoys and other non-ship data based on the assumption that these generally measure relative
462 humidity directly. For any ship observations with no exposure information we apply 55 % of the 3.4 %
463 adjustment based on the mean percentage of observations with EOH metadata that require an adjustment over
464 the 1973-2014 (metadata) period). This partial adjustment factor follows the method of Berry and Kent (2011)
465 and Josey et al. (1999) but differs in quantity. They assessed this over a shorter time period and found then that
466 ~ 30 % of observations were from poorly ventilated instruments.

467

468 To estimate the uncertainty in the non-aspirated instrument adjustment applied U_i , we use the Berry and Kent
469 (2011) and Josey et al. (1999) uncertainty estimate of 0.2 g kg^{-1} and apply this in all cases where an adjustment
470 or partial adjustment has been applied. This is treated as a standard uncertainty (1σ). In the case of partial
471 adjustments for the ship observations with no metadata there is large uncertainty in both the adjustment and
472 adjusted value. To account for this we use the amount of what would have been a full 3.4 % adjustment in
473 addition to the 0.2 g kg^{-1} as the 1σ uncertainty.

474

475 To carry these adjustments and uncertainties to all other humidity variables we start with q and then propagate
476 the adjusted quantity and adjusted quantity plus uncertainty using the equations in Table S1. Using the original
477 T (which does not need to be adjusted for poor ventilation) and ERA-Interim climatological surface pressure, e
478 can be calculated from q . T_d and RH can be calculated from e and T . From these, the T_w and DPD can be

479 calculated. The uncertainty is then obtained by subtracting the adjusted quantity from the adjusted quantity plus
480 uncertainty for each variable.

481

482 3.3.2 Application of adjustments for biases from ship heights

483

484 After bias adjustment for poor ventilation, all variables are adjusted to approximately 10 m elevation. This
485 serves to account for the inhomogeneity from the systematic increase in ship height over time and for spatial
486 inhomogeneity between observations made at different heights. In the absence of height adjustments, increasing
487 ship heights likely lead to a small decrease in air temperature and specific humidity over time (Berry and Kent,
488 2011) because these quantities generally decrease with height. As Fig. 3 shows, the standard deviations in ships'
489 instrument heights exceed 5 m in most cases. Also, we have included buoys in the processing so far and these
490 can be very low (~4 m, e.g. Gilhousen, 1987) relative to ship observing heights.

491

492 The height of the hygrometer (HOH) must be estimated (HOHest) as no metadata is available. In the case of
493 psychrometers, which are the most common instruments listed in the ship metadata, the wet and dry bulb
494 thermometers are co-located. Figure 3 shows that the visual observation height (HOP) is the most commonly
495 available information, followed by the barometer height (HOB) and then thermometer height (HOT). It also
496 shows the mean and standard deviation of all observing heights including the anemometer (HOA). Hence,
497 HOHest is obtained using the following methods in preference order:

498

- 499 1. HOP present and >2 m: HOHest $\mu = \text{HOP}$, $\sigma = 1$ m
- 500 2. HOB present and >2 m: HOHest $\mu = \text{HOB}$, $\sigma = 1$ m
- 501 3. HOT present and >2 m: HOHest $\mu = \text{HOT}$, $\sigma = 1$ m
- 502 4. HOA present and >12 m: HOHest $\mu = \text{HOA} - 10$, $\sigma = 9$ m
- 503 5. No height metadata: HOHest $\mu = 16$ m + the linear trend in mean HOP/HOB/HOT height to the
504 date of observation, $\sigma = 4.6$ m + the linear trend in standard deviation HOP/HOB/HOT height to
505 the date of observation

506

507 The μ and σ of the combined HOP, HOB and HOT increases from 16 m and 4.6 m respectively in January 1973
508 to 23 m and 11 m respectively in December 2014. Kent et al. (2007) and Berry and Kent (2011) used 16 m to 24

509 m between 1971 and 2007 so our estimate is very similar. The anemometer height is also required for the
 510 adjustments. We either use the provided HOA as long as it is greater than 2 m or set it to 10m above the
 511 HOHest. All buoys are assumed to be observing at 4 m, with anemometers at 5 m
 512 (<http://www.ndbc.noaa.gov/bht.shtml>).

513

514 Once HOHest has been obtained for each observation, the air temperature and specific humidity are adjusted to
 515 10 m using bulk flux formulae. The methodology, assumptions and parameterisations largely follow that of
 516 Berry and Kent (2011), Berry (2009), Smith (1980, 1988) and Stull (1988). Essentially, the quantity of interest x
 517 can be adjusted to a reference height of 10 m as follows:

518

$$519 \quad x_{10} = x - \frac{x_*}{\kappa} \left(\ln \left(\frac{z_x}{10} \right) - \psi_x + \psi_{x10} \right) \quad (1)$$

520

521 where x_* is the scaling parameter specific to that variable (e.g., friction velocity in the case of u , characteristic
 522 temperature or specific humidity in the case of T or q respectively), κ is the von Karman constant (0.41 used
 523 here), z_x is the observation height of the variable of interest, ψ_x is the stability correction for the variable of
 524 interest and is a function of z_x/L , ψ_{x10} is the stability correction for the variable of interest at a reference height of
 525 10m and is a function of $10/L$ and L is the Monin-Obukov Length.

526

527 An iterative approach (as done for Berry and Kent 2011) is required to resolve Eq. (1) because we only have
 528 basic meteorological variables available at a single height for each observation. We start from T , q , u , sea
 529 surface temperature (SST), the co-located 1° by 1° gridbox pentad climatological surface pressure from ERA-
 530 Interim (climP), HOHest which becomes both z_q and z_t and our estimated anemometer height which becomes z_u .
 531 For some observations the SST or u is missing. If SST is missing it is given the same value as T so in effect, no
 532 adjustment to T is applied. Either way, the SST is set to a minimum of -2° C and a maximum of 40° C. If u is $<$
 533 0.5 m s^{-1} it is given a light wind speed of 0.5 m s^{-1} . If u is missing or $>100 \text{ m s}^{-1}$ it is assumed to be erroneous but
 534 given a moderate wind speed of 6 m s^{-1} . We also approximate surface values T_0 , q_0 and u_0 where $T_0 = \text{SST}$, $q_0 =$
 535 $q_{sat}(\text{SST}) * 0.98$ and $u_0 = 0$. Clearly, with so many necessary approximations there are many different plausible
 536 methodological choices, hence the need for multiple independent analyses that explore these different choices in
 537 order to quantify the structural uncertainty.

538

539 We begin the iteration by assuming a value for L depending on assumed stability:

540 - if $(SST - T) > 0.2$ °C: $L = -50$ m, unstable conditions are assumed;

541 - if $(SST - T) < -0.2$ °C: $L = 50$ m, stable conditions assumed;

542 - if $(SST = T) \pm 0.2$ °C: $L = 5000$ m, neutral conditions assumed where L tends to ∞ .

543 We also start with an assumption that the 10 m wind speed in neutral conditions $u_{10n} = u$. The iteration is
544 continued until L converges to within 0.1 m, which it generally does. If after 100 iterations there is no
545 convergence we either apply no adjustment or if absolute L is large (> 500 m) we assume neutral conditions and
546 take L (and all other parameters) as they are. In cases where u_* is very large (it should be < 0.5 m s⁻¹ [Stull,
547 1988]) we also apply no adjustment. The iteration involves 21 steps as described in the Supplementary Material.
548

549 For most observations we arrive at a plausible L , friction velocity u_* , ψ_x and ψ_{x10} . We then calculate the scaling
550 parameters T_* and q_* :

551

552
$$T_* = \kappa \left(\ln \left(\frac{z_t}{z_{t0}} \right) - \psi_t \right)^{-1} (T - T_0) \quad (2a)$$

553
$$q_* = \kappa \left(\ln \left(\frac{z_q}{z_{q0}} \right) - \psi_q \right)^{-1} (q - q_0) \quad (2b)$$

554

555 where the neutral stability heat transfer coefficient $z_{t0} = 0.001$ m and the neutral stability moisture transfer
556 coefficient $z_{q0} = 0.0012$ m (Smith 1988). The adjusted values for T_{10} and q_{10} can then be calculated from Eq. (1).
557 From these we recalculate the other humidity variables using the equations in Table S1.

558

559 There is uncertainty in the obtained HOHest. Given that this is a best estimate we assume that the uncertainty in
560 the height is normally distributed and use the standard deviation in the height estimate HOHest to calculate an
561 uncertainty range in the height adjusted value x (where x is any of T , q etc.) of xH_{min} to xH_{max} . Following the
562 ‘two out of three chance’ rule in the BIPM Guide to the Expression of Uncertainty in Measurement (BIPM,
563 2008), the standard uncertainty (1σ) for the height adjusted value (U_h) is then given by:

564

565
$$U_h = \frac{xH_{max} - xH_{min}}{2} \quad (3)$$

566

567 The range xH_{min} to xH_{max} depends on the source of HOHest and associated σ , as listed above. There are several
568 scenarios where estimating the uncertainty in this way is not possible or calculation of an adjustment is not
569 possible. Also, U_h for buoys is highly uncertain given the lack of height information available. These alternative
570 scenarios are documented in Table 2.

571

572 **3.4 Estimating residual uncertainty at the observation level**

573

574 Three other sources of uncertainty affect the marine humidity data at the observation level. These are
575 measurement uncertainty U_m , climatology uncertainty U_c and whole number uncertainty U_w . These are all
576 assessed as 1 σ standard uncertainties.

577

578 We have estimated U_m for each observation following the method used for HadISDH.land (Willett et al., 2013,
579 2014). This assumes that humidity was measured using a psychrometer which is a reasonable assumption for the
580 marine ship data (Fig. 4). The HadISDH.land measurement uncertainty is based on an estimated standard (1 σ)
581 uncertainty in the wet bulb and dry bulb instruments of 0.15° C and 0.2° C respectively. As shown in Table S3,
582 the equivalent uncertainty for the other variables depends on the temperature. The uncertainty is applied as a
583 standard uncertainty in RH depending on which bin the air temperature falls in. This is then propagated through
584 the other variables starting with vapour pressure, using the equations in Table S1.

585

586 Whole numbers of air and/or dew point temperature that have either been flagged as such during quality control
587 (Sect. 3.2), or that belong to a source deck/year where whole numbers make up more than two times the
588 frequency of other decimal places (Table S4), are given an uncertainty U_w . These decks and years where whole
589 numbers are very common differ for air and/or dew point temperature. Clearly with so many decks affected, the
590 removal of entire decks to remove any whole number biasing could easily reduce sampling to critically low
591 levels. We cannot distinguish between observations that have been rounded versus those that have been
592 truncated so we assume that all offending whole numbers have been rounded. This means that the value could
593 be anywhere between $\pm 0.5^\circ$ C, with a uniform distribution. Hence, where only air or dew point temperature is
594 an offending whole number the standard 1 σ uncertainty expressed in air or dew point temperature ($^\circ$ C) is:

595

596
$$U_w = \frac{0.5}{\sqrt{3}} \tag{4}$$

597

598 Where both air and dew point temperature are offending whole numbers the standard 1σ uncertainty expressed
599 in air or dew point temperature ($^{\circ}\text{C}$) for dew point depression, relative humidity and wet bulb temperature is:

600

601
$$U_w = \frac{1}{\sqrt{3}} \tag{5}$$

602

603 There is uncertainty U_c in the climatological values used to calculate climate anomalies because of missing data
604 over time, uneven and sparse sampling in space and also the inevitable mismatch between a point observation
605 and a 1° by 1° gridded pentad climatology. This uncertainty reduces with the number of observations
606 contributing to the climatology N_{obs} and with the variability of the region σ_{clim} . The climatologies used to create
607 the anomalies have undergone spatial and temporal interpolation to move from 5° by 5° gridded monthly
608 climatologies and climatological standard deviations σ_{clim} to maximise coverage and so it is not straightforward
609 to assess the number of observations contributing to each 1° by 1° gridded pentad climatology and the true σ_{clim}
610 is likely greater. The minimum number of years required to be present over the 30 year climatology period is 10.
611 Therefore, we assume a worst case scenario of $N_{obs} = 10$. Hence, for a standard 1σ uncertainty:

612

613
$$U_c = \frac{\sigma_{clim}}{\sqrt{N_{obs}}} \tag{6}$$

614

615 **3.5 Gridding of actual and anomaly values and uncertainty**

616

617 To create a quasi-global monitoring product the raw observations need to be gridded. The spatial density is too
618 low for high resolution grids and the intended purpose is for this marine product to be blended with the
619 HadISDH.land humidity product which is on a 5° by 5° grid at monthly resolution. Hence, the point hourly
620 observations must be averaged to monthly mean gridded values.

621

622 The sparsity of the data means that there is a risk of bias due to poor sampling. A 5° by 5° gridbox covers an
623 area greater than 500 km^2 by 500 km^2 which, despite the large correlation decay distances of both temperature
624 and humidity, can include considerable variability. Furthermore, a monthly mean can be made up of a strong
625 diurnal cycle and considerable synoptic variability. This is minimised by the use of climate anomalies but

626 regardless, care should be taken to ensure sufficient sampling density while maximising coverage where
627 possible.

628

629 Several data-density criteria were trialled to balance spatial coverage and poor representativeness (high
630 variance) of the gridbox averages. Climate anomalies are created at the raw observation level by subtracting the
631 nearest 1° by 1° pentad climatology (1981-2010) and so we can grid both the actual values and the anomalies.
632 Gridding of the anomalies is safer than gridding actual values in terms of biasing through poor sampling density
633 because the correlation length scales of anomalies are higher than for actual temperatures. Initially, ERA-
634 Interim is used to provide a climatology. This then requires an iterative approach to produce an initial
635 observation-based climatology and improve the climatology through quality control. To reduce biasing further
636 we grid the data in six stages to create an average at each stage. The entire process including quality control,
637 bias adjustment, gridding and three iterations, is shown diagrammatically in Fig. 5 and each gridding stage
638 described below.

639

- 640 1. Create 1° by 1° 3-hourly gridded means of the hourly observations of actuals and anomalies; there
641 must be at least one observation.
- 642 2. Create separate 1° by 1° daytime and night time gridded means of the 1° by 1° 3-hourly gridded
643 mean actuals and anomalies; there must be at least one 1° by 1° 3-hourly grid.
- 644 3. Create 5° by 5° monthly daytime and night time gridded means of the 1° by 1° daytime and night
645 time gridded mean actuals and anomalies; there must be at least 0.3*days in the month of 1° by 1°
646 daily grids.
- 647 4. Create combined 5° by 5° monthly gridded means of the 5° by 5° monthly daytime and night time
648 gridded mean actuals and anomalies; there must be at least 1 5° by 5° monthly daytime or night
649 time gridded mean.
- 650 5. Create 1981-2010 5° by 5° monthly mean climatologies and standard deviations from the 5° by 5°
651 monthly gridded means of actuals and anomalies; there must be at least 10 5° by 5° monthly
652 gridded means.
- 653 6. Renormalise the gridded anomalies by subtracting the monthly anomaly 1981-2010 climatology to
654 remove biases from use of the previous iteration climatology (Sect. 4.1).

655

656 At each iteration the gridded observation based climatologies are infilled linearly over small gaps in space and
 657 time and then interpolated down to 1° by 1° pentad resolution. The observations are too sparse to create such
 658 high-resolution grids directly.

659

660 The observation uncertainties also need to be gridded and the total observation uncertainty U_o calculated. Ships
 661 move around, and so their uncertainties also track around the globe. This means that the uncertainty in any one
 662 point / gridbox bears some relationship to nearby points / gridboxes over time and space and cannot be treated
 663 independently. Correlation needs to be accounted for both in gridding and subsequently creating regional
 664 averages from gridboxes to avoid underestimation. The five sources of observation uncertainty are summarised
 665 in Table 2. The non-aspirated instrument adjustment uncertainty U_i , height adjustment uncertainty U_h and
 666 climatology uncertainty U_c persist over time and space as ships move around. These are accordingly treated as
 667 correlating completely within one gridbox month. The measurement uncertainty U_m , and whole number
 668 uncertainty U_w are likely to differ observation to observation and so treated as having no correlation within one
 669 gridbox month. Hence, observation uncertainty sources are first gridded individually, following the first four
 670 steps outlined above and taking into account correlation where necessary. For those that do not correlate (U_m
 671 and U_w) the gridbox mean uncertainties U_{gb} for each source are combined over N points in time and space as
 672 follows:

673

$$674 \quad U_{gb} = \frac{\sqrt{a^2+b^2\dots+n^2}}{N} \quad (7)$$

675

676 For those sources that do correlate (U_c , U_i and U_h), assuming $r = 1$, the gridbox mean uncertainties U_{gb} for each
 677 source are combined over N points in time and space as follows:

678

$$679 \quad U_{gb} = \frac{a+b\dots+n}{N} \quad (8)$$

680

681 To create the total observational uncertainty for each gridbox the gridbox quantities of the five uncertainty
 682 sources can then be combined in quadrature:

683

$$684 \quad U_o = \sqrt{U_c^2 + U_m^2 + U_w^2 + U_h^2 + U_i^2} \quad (9)$$

685

686 Given the general sparsity of observations across each gridbox month and the uneven distribution of
687 observations across each gridbox and over time there is also a gridbox sampling uncertainty component, U_s .
688 This is estimated directly at the 5° by 5° monthly gridbox level and follows the methodology applied for
689 HadISDH.land (Willett et al., 2013, 2014), denoted SE^2 , which is based on station-based observations from
690 Jones et al (1997):

691

$$692 \quad U_s = \frac{(\bar{s}_i^2 \bar{r}(1-\bar{r}))}{(1+(N_s-1)\bar{r})} \quad (10)$$

693 .

694 where \bar{s}_i^2 is the mean variance of individual stations within gridbox, \bar{r} is the mean inter-site correlation and N_s is
695 the number of stations contributing to the gridbox mean in each month. The mean variance of individual stations
696 within the gridbox is estimated as:

697

$$698 \quad \bar{s}_i^2 = \frac{(\hat{S}^2 N_{SC})}{(1+(N_{SC}-1)\bar{r})} \quad (11)$$

699

700 where \hat{S}^2 is the variance of the gridbox monthly anomalies over the 1982-2010 climatology period and N_{SC} is
701 the mean number of stations contributing to the gridbox over the climatology period. The mean inter-site
702 correlation is estimated by:

703

$$704 \quad \bar{r} = \frac{x_0}{X} \left(1 - \exp\left(-\frac{x_0}{X}\right) \right) \quad (12)$$

705

706 where X is the diagonal distance across the gridbox and x_0 is the correlation decay length between gridbox
707 means. We calculate x_0 as the distance (gridbox midpoint to midpoint) at which correlation reduces to 1/e. To
708 account for the fact that marine observations generally move around at each time point we use the concept of
709 pseudo-stations to modify this methodology. For any one day there could be 25 1° by 1° gridboxes and so we
710 assume that the maximum number of pseudo-stations per gridbox is 25 which is broadly consistent with the
711 number of stations per gridbox in HadISDH.land. Over a month then, there could be a maximum of 775 1° by 1°
712 daily gridboxes contributing to each 5° by 5° monthly gridbox. Given ubiquitous missing data and sparse
713 sampling the maximum in practice is closer to 600. Using these values we then scale the actual number of 1° by

714 1° daily gridboxes contributing to each 5° by 5° monthly gridbox to provide a pseudo-station number between 1
715 and 25 for each month (N_s) and then the average over the climatology period (N_{SC}).

716

717 The gridbox U_o and U_s uncertainties are then combined in quadrature, assuming no correlation between the two
718 sources. This gives the full gridbox uncertainty U_f . Calculation of regional average uncertainty and spatial
719 coverage uncertainty is covered in Sect. 4.

720

721 **4 Analysis and validity of the gridded product**

722

723 The final gridded marine humidity monitoring product presented as HadISDH.marine.1.0.0.2018f is the result of
724 the 3rd iteration quality-control and bias-adjustment of ship-only observations average into 5° by 5° gridded
725 monthly means (Fig. 5). There are four reasons for only using the ship observations. Firstly, the increase in
726 spatial coverage in the combined ship and buoy product is actually fairly small (Fig. S2) and only during the
727 latter part of the record. Secondly, a dataset intended for detecting long-term changes in climate should have
728 reasonably consistent input data and coverage over time. Thirdly, we believe that the buoy data are less reliable
729 given their proximity to the sea surface and exposure to sea spray contamination in addition to the lower
730 maintenance frequency compared to ship data. Fourthly, there are no metadata available for buoy observations
731 which makes it difficult to apply necessary bias adjustments or estimate uncertainties. Actual monthly means,
732 anomalies from the 1981-2010 climatology (not standardised by division with the standard deviation), the
733 climatological means and standard deviation of the climatologies, uncertainty components and number of
734 observations for both products are all made available as netCDF from www.metoffice.gov.uk/hadobs/hadisdh/.

735

736 **4.1 Comparison of climatologies between HadISDH.marine and ERA-Interim**

737

738 At the end of each iteration (Fig. 5), observation-based climatology fields are created at both the monthly 5° by
739 5° grid and, by interpolation, pentad 1° by 1° grid (Sect. 3.5). These are then used to quality control and create
740 anomaly values for the next iteration. Hence, the 2nd iteration quality-controlled data are used to build the final
741 3rd iteration and therefore, there should be no lasting effect from having used the ERA-Interim fields initially.
742 The quality-controlled, buddy-checked and bias-adjusted 3rd iteration is used to create the final climatology
743 provided to users.

744

745 To compare the use of ERA-Interim versus the observation based climatology to calculate anomalies and quality
746 control the data we show difference maps of the 2nd iteration minus ERA-Interim pentad 1° by 1° grid
747 climatologies and climatological standard deviations in Figs. S9 to S14 for a selection of pentads and variables.
748 Note that ERA-Interim fields are for 2 m above the ocean surface whereas the raw observations range between
749 approximately 10 m to 30 m above the surface. In normal conditions we may therefore expect ERA-Interim to
750 provide climatologies that are warmer and moister than the observations. However, overall, ERA-Interim
751 appears drier (both in absolute and relative terms) and cooler than the observation based climatologies. For
752 humidity this is consistent with the results of Kent et al. (2014). For the majority of gridboxes these differences
753 are within $\pm 2 \text{ g kg}^{-1}$, %rh and °C. However, differences are especially strong around coastlines with
754 magnitudes exceeding $\pm 10 \text{ g kg}^{-1}$, %rh and °C. This is to be expected given that ERA-Interim coastal
755 gridboxes will include effects from land, especially at the relatively coarse 1° by 1° grid resolution. For relative
756 humidity there are more regions where ERA-Interim is more saturated and there is more seasonality in the
757 differences. Relative humidity is less stable spatially and on synoptic time scales and also more susceptible to
758 biases and errors than specific humidity and air temperature, largely because it is affected by errors in both air
759 temperature and dew point temperature. For temperature, the coastal difference can be positive or negative
760 depending on the season.

761

762 The climatological standard deviations are generally lower in the 2nd iteration observations compared to ERA-
763 Interim. Differences are generally between $\pm 2 \text{ g kg}^{-1}$, %rh and °C but for relative humidity there are expansive
764 regions in the extratropics to mid-latitudes, especially in the Northern Hemisphere where climatological
765 standard deviations are up to 5 %rh lower in the observations. The generally lower variability in the
766 observation-based climatology is to be expected given the interpolation from monthly mean resolution and
767 interpolation over neighbouring gridboxes where data coverage is limited. However, much of the tropics,
768 particularly in the Southern Hemisphere tends to show more variability in the observations. Similarly, many of
769 the peripheral gridboxes (those at the edge of the spatial coverage and therefore more likely to be interpolated
770 from nearby gridboxes rather than based on actual data) show higher variability for specific and relative
771 humidity and lower variability for air temperature. All of these gridboxes are in data sparse regions which likely
772 contributes to the higher variability. Ideally, observation based climatologies would be created directly at the

773 pentad 1° by 1° grid but this severely reduces spatial coverage of the climatology fields and any product based
774 on them. A balance has to be made between coverage and quality.

775

776 Annual mean 5° by 5° climatologies (no interpolation) from the 3rd iteration quality-controlled, bias-adjusted
777 ship-only product are shown in Fig. 7 for specific humidity, relative humidity, air temperature and dew point
778 temperature. These have a minimum data presence threshold of 10 years for each month over the climatology
779 period and at least 9 climatological months present for the annual climatology. Data coverage is virtually non-
780 existent in the Southern Hemisphere below 40° S and Northern Hemisphere coverage diminishes drastically
781 above 60° N. These climatologies are as expected for these variables and compare well in terms of broad spatial
782 patterns with ERA-Interim (not shown). There is good spatial consistency considering that no interpolation has
783 been conducted meaning that any erroneous gridboxes should stand out. We conclude that as a first version
784 product, these climatologies look reasonable.

785

786 **4.2 Analyses of global averages for various processing stages and with other products**

787

788 Global average quantities are key measures of climate change and so we focus here on the differences arising
789 from the various processing steps of HadISDH.marine along with the NOCSv2.0 specific humidity and ERA-
790 Interim reanalysis products. Global averages have been created by weighting each gridbox by the cosine of its
791 latitude at gridbox centre. All timeseries shown are the renormalised anomalies with a zero-mean over the 1981-
792 2010 period. Figs. 8 to 11 show timeseries for specific humidity, relative humidity, dew point temperature and
793 air temperature respectively. Decadal linear trends (shown) are computed using ordinary least squares regression
794 with ranges representing the 90th percentile confidence interval calculated using AR(1) correction (Santer et al.,
795 2008).

796

797 For all variables, there are only small differences in the global average timeseries between the various
798 processing steps – from the raw data (noQC) to the 3rd iteration quality-controlled (noBA [no bias adjustment])
799 and then the bias-adjusted data (BA). They are smallest for air temperature and largest for relative humidity but
800 all steps result in global average trends that are significant and in the same direction, and have similar
801 interannual variability. We consider these trends to be significant because the 90th percentile confidence
802 intervals around the trend are not large enough to bring the direction of the trends into question. The trends in

803 the global average are positive over the 1973-2018 period for specific humidity, dew point temperature and air
804 temperature, and negative for relative humidity. The linear trends for the final HadISDH.marine.1.0.0.2018f
805 version are $0.07 \pm 0.02 \text{ g kg}^{-1} \text{ decade}^{-1}$, $-0.09 \pm 0.08 \text{ \%rh decade}^{-1}$, $0.09 \pm 0.02^\circ \text{ C decade}^{-1}$ and $0.11 \pm 0.03^\circ \text{ C}$
806 decade^{-1} for specific humidity, relative humidity, dew point temperature and air temperature respectively.
807 Hence, we conclude that HadISDH.marine shows moistening and warming since the 1970s globally in actual
808 terms but that the air above the oceans appears to have become less saturated and drier in relative terms. This
809 differs from theoretical expectation where changes in relative humidity over ocean are strongly energetically
810 constrained to be small, of the order of $1\% \text{ K}^{-1}$ or less, and generally positive (Held and Soden, 2006; Schneider
811 et al., 2010). Model-based expectations also suggest small positive changes (Byrne and O’Gorman, 2013, 2016,
812 2018). Despite careful quality control and bias-adjustment the previously noted moist humidity bias pre-1982 is
813 still apparent in the bias-adjusted (BA) data. The linear trend in relative humidity from 1982 to 2018 is $-0.03 \pm$
814 $0.13 \text{ \%rh decade}^{-1}$, and therefore not significantly decreasing which is more consistent with expectation.
815
816 Since there are considerable known issues affecting the marine humidity data, and because there are large
817 outliers (Figs. S3 to S6), the effect of quality (noQC compared to noBA), might be expected to be large.
818 Furthermore, approximately 25 %, dropping steadily over time to 18 % of the initial selection of data have been
819 removed by the quality control (Fig. 5), so there is a considerable difference in the amount of data contributing
820 to the quality-controlled version compared to the raw version. Despite all of this, differences are relatively
821 small. Overall, the quality control makes the positive trends smaller (specific humidity, dew point temperature
822 and air temperature) and negative trends larger (relative humidity). The effect of quality control, including
823 buddy checking, is largest in the 1970s to early 1980s, when the largest amount of data was removed by quality
824 control. This is especially noticeable for relative humidity and dew point temperature, suggesting that the pre-
825 1982 bias, although present to some extent in the raw (noQC) data, could be exacerbated by the quality control.
826 This could be due to erroneous removal of good data but investigation (Figs. S3 to S8) suggests that much of the
827 data removal was appropriate – many very low relative humidity values were removed. It could also be an
828 artefact of the reduced number of observations after quality control, reducing the chance of averaging out
829 random error. To explore whether the presence of whole numbers in the record has contributed to the pre-1982
830 bias we have processed a bias adjusted version with all whole number flagged data (Table 1) removed
831 (BA_no_whole) which is shown against the noQC and BA versions in Fig. 9d. The resulting global average
832 trend is largest in the BA_no_whole version, even over the 1982-2018 period, and the pre-1982 bias is still

833 clear. We conclude that the pre-1982 moist bias remains apparent in HadISDH.marine, and is not yet well
834 understood, and quality control of the pre-1982 data is an area for more research in future versions.

835

836 The bias adjustment (BA, BA_HGT, BA_INST) reduces the negative trends in relative humidity compared to
837 the quality-controlled (noBA) data, and increases the positive trends in specific humidity and dew point
838 temperature relative to the quality-controlled data. The effect of bias adjustment is negligible for air
839 temperature, which only has adjustment for ship height applied. For the humidity variables the height
840 adjustment has a far larger effect than the non-aspirated instrument adjustment. The non-aspirated instrument
841 adjustment makes the positive trends in specific humidity and dew point temperature slightly smaller and the
842 negative trends in relative humidity slightly larger. The height adjustment has the opposite effect. For relative
843 humidity, the bias adjustments appear to have introduced greater intra-decadal scale variability but retained the
844 interannual patterns, again highlighting the sensitivity of relative humidity compared to the other variables.
845 Given that these biases exist we do have to try and mitigate their impact. However, this is a focus area for
846 investigation and improvements in future versions of HadISDH.marine.

847

848 The timeseries that include data from moored buoys compared to those from ships only ('all' versus 'ship')
849 show smaller positive trends for specific humidity and air temperature and larger negative trends for relative
850 humidity. Moored buoys begin to play a role from the late 1980s, increasing in number dramatically to make up
851 over 50 % of the observations by 2015. The 'all' timeseries can be seen to diverge slightly from the 'ship'
852 timeseries in the latter part of the record. Therefore, it is more consistent to produce the final HadISDH.marine
853 version without inclusion of moored buoy data.

854

855 Before quality control there are more daytime ship observations than night time ship observations in the early
856 record (~1 000 000 compared to ~800 000 per year) but this evens out by the end of the record to ~900 000 per
857 year. However, the quality control removes more daytime observations than night time observations, especially
858 in the 1970s and 1980s such that both contribute ~700 000 observations per year, dipping in the middle of the
859 record. There has been no bias adjustment for solar heating of ships applied in this version of HadISDH.marine
860 so the daytime data may contain some artefacts of solar heating. If this is a problem it should affect the air
861 temperature and relative humidity but not the dew point temperature or specific humidity (Sect. 2.1). While the
862 full dataset (both) combines both daytime and night time data, for various gridboxes and seasons there is only

863 either a daytime or night time value present. As such, the ‘both’ timeseries and its linear trend may not be a
864 straightforward average of the ‘day’ and ‘night’ timeseries and trends. For specific humidity, dew point
865 temperature and air temperature the ‘day’ and ‘night’ trend differences are essentially negligible, with linear
866 trends identical or within $0.01 \text{ g kg}^{-1} \text{ decade}^{-1}$. Even for relative humidity the differences are small. The ‘day’
867 timeseries gives the largest negative trend followed by ‘both’ which is $0.01 \text{ \%rh decade}^{-1}$ smaller and then
868 ‘night’ which is $0.02 \text{ \%rh decade}^{-1}$ smaller again. The negligible differences in air temperature suggest that
869 solar heating is not a significant concern at least at the global average scale. Relative humidity is very sensitive
870 to any differences in the data but even these differences are fairly small and do not change the overall
871 conclusion of decreasing full-period trends and no significant trend over the 1982-2018 period. ‘Night’ trends
872 are often thought to provide a better signal of change because they are generally free from convective and
873 shortwave radiative processes and more a measure of outgoing longwave radiation. The main conclusion here is
874 that trends and variability are very similar in the daytime, night time and combined timeseries which adds
875 confidence in their representativeness of real-world trends and variability.

876

877 In terms of linear trend direction, HadISDH.marine compares well with other monitoring estimates from
878 NOCSv2.0 and ERA-Interim and to other reanalyses and older products (Fig. 1). ERA-Interim in Figs. 8 to 11 is
879 from analysis fields of 2 m air temperature and dew point temperature and has been masked to ocean coverage
880 using a 1° by 1° land-sea mask and also to HadISDH.marine coverage for comparison. Note that the ERA-
881 Interim timeseries shown in Fig. 1 are from background forecast values to avoid biases introduced from ship
882 data and ocean-only points over open sea. Both NOCSv2.0 and HadISDH.marine are estimates of 10 m
883 quantities and the NOCSv2.0 coverage is similar to that of HadISDH.marine but it only extends to 2015.
884 NOCSv2.0 shows the largest trends in specific humidity over the 1979-2015 common period, $0.04 \text{ g kg}^{-1} \text{ decade}$
885 $^{-1}$ greater than HadISDH.marine. The interannual patterns are broadly similar but with some differences showing
886 that methodological choices do make a difference, given that the underlying observations are from the same
887 source. ERA-Interim shows very weak moistening compared to HadISDH.marine for specific humidity and dew
888 point temperature and slightly weaker warming for air temperature. Over the longer 1979-2018 period ERA-
889 Interim trends are slightly larger for specific humidity but still weaker than in HadISDH.marine. The decreasing
890 saturation in relative humidity is very strong in ERA-Interim at more than 2 times the HadISDH.marine trend
891 over the common period. The masking to HadISDH.marine coverage surprisingly makes very little difference in
892 the linear trends, they are slightly more negative, and only small year-to-year differences. Interannual behaviour

893 does differ, especially for relative humidity and especially in the period up to the early 1990s where ERA-
894 Interim is warmer and wetter generally, thus moderating the long-term trends in specific humidity, dew point
895 temperature and air temperature. Note that the ERA-Interim background field relative humidity shown in Fig. 1
896 also shows a decrease but to a lesser extent than the analysis fields (Fig. 9) which include ship data. Agreement
897 is closest for air temperature in both trends and variability.

898

899 The decreasing relative humidity trends over ocean are similar to the drying seen in HadISDH.land and ERA-
900 Interim land relative humidity (Fig. 1); land linear trends are 0.03 %rh more negative at -0.12 (-0.27 to -0.03)
901 %rh 10 yr⁻¹ over the same 1973 to 2018 period. The timeseries pattern is quite different though with marine
902 relative humidity decreasing throughout the period around large variability and land relative humidity clearly
903 decreasing from 2000. The greater sensitivity of relative humidity to observation errors, biases and sampling
904 issues makes the conclusion of long-term drying an uncertain one but agreement with ERA-Interim adds some
905 weight to this conclusion.

906

907 For the final HadISDH.marine.1.0.0.2018f product the regional average uncertainty is also computed and shown
908 for the global average (70° S to 70° N) in Fig. 12. This includes the total observation uncertainty, which covers
909 uncertainty components for instrument adjustment, height adjustment, measurement, climatology and whole
910 number uncertainty (Table 2). In addition, the regional average uncertainty includes the gridbox sampling
911 uncertainty and also a spatial coverage uncertainty, following the method applied for HadISDH.land (Willett et
912 al., 2014). The coverage uncertainty essentially uses the variability between ERA-Interim full coverage
913 compared to ERA-Interim with HadISDH.marine coverage to estimate uncertainty. To obtain uncertainty in the
914 global average from the gridbox uncertainties correlation in time and space should be taken into account. It is
915 not trivial to assess the true spatial and temporal correlation of the various uncertainty sources. In reality,
916 although ships move around over space and time, implying some correlation, the contributing sources to each
917 ~500 km² gridbox monthly mean differ widely. Therefore, for this first version product we assume no
918 correlation between gridboxes in time or space and take the simple approach of the quadrature combination of
919 uncertainty sources, noting that this is a lower limit on uncertainties.

920

921 The uncertainty in the global averages (Fig. 12) is larger than the equivalent timeseries for land (see Fig. 12 in
922 Willett et al., 2014). The coverage uncertainty (accounting for observation gaps in space and time) is generally

923 the largest source of uncertainty with the exception of relative humidity and dew point depression. For the latter
924 two, the total observation uncertainty makes up the greatest contribution. In all cases the total observation
925 uncertainty is larger at the beginning and especially the end of the records, where there are fewer/no metadata
926 with which to apply bias adjustments. The contribution from sampling uncertainty (gridbox spatial and temporal
927 coverage) is generally very small except for relative humidity. This is as expected given that the correlation
928 decay distance of humidity should generally be larger over ocean than over land given the homogeneous surface
929 altitude and composition. Overall, the magnitudes of the uncertainties are small relative to the magnitudes of
930 long-term trends and variability in all variables except for relative humidity and dew point depression. This
931 suggests that there is good confidence in changes in absolute measures of humidity over ocean (e.g., specific
932 humidity), and also air temperature, but lower confidence in changes in the relative humidity. The warming and
933 moistening are further corroborated by strong theoretical reasoning based on laws of physics governing the
934 expectation that specific humidity should have increased over the period of record given the warming of the
935 oceans and atmosphere that has occurred (Hartmann et al., 2013). The uncertainty model makes many
936 assumptions over correlation of uncertainty in space and time. It is likely that we have overestimated the
937 uncertainty at the gridbox scale by assuming complete correlation for height adjustment uncertainty, instrument
938 adjustment uncertainty and climatological uncertainty. Conversely, we have likely underestimated the
939 uncertainty at the regional average level by assuming no correlation. This is certainly an area for improvement
940 in future versions.

941 **4.3 Decadal trends across the globe presented by HadISDH.marine**

942

943 Figure 13 shows the decadal linear trends for specific humidity, relative humidity, dew point temperature and air
944 temperature for HadISDH.marine.1.0.0.2018f. The completeness criteria for trend fitting is 70 %, more strict
945 than for the climatologies (Fig. 7). This results in poorer spatial coverage especially in the Southern
946 Hemisphere. Clearly, there are no data points outside 70° S to 70° N, hence the restriction of the global average
947 timeseries to this region is sensible. The tropical and Southern Hemisphere Pacific Ocean, and Southern
948 Hemisphere Atlantic Ocean have virtually no data coverage. Overall, the appearance of the trends shows good
949 spatial consistency, with few gridboxes standing out as obviously erroneous. There has been no interpolation
950 across gridboxes that would have smoothed out any outliers, and so the lack of these outlying gridboxes
951 suggests that the data are of reasonable quality for this long-term analysis at least. Trends are as expected from

952 the global average timeseries – generally moistening and warming but becoming less saturated. The same is true
953 over land (Willett et al., 2014).

954

955 The moistening shown in specific humidity and dew point temperature (Fig. 13 panels a, b and e, f) is
956 widespread. The majority of gridboxes are considered to be statistically significant in that the 90th percentile
957 confidence interval around the trend magnitude is the same sign as the trend and does not encompass zero. The
958 largest increases in specific humidity are in the lower latitudes whereas the largest increases in dew point
959 temperature are more spread out with a tendency towards the extratropics and mid-latitudes. There are a few
960 regions where there are clusters of gridboxes with drying trends. These are generally consistent between the
961 specific humidity and dew point temperature, especially in the few cases where these negative trends are
962 significant such as the central Pacific, the east coast of Brazil, the southern coast of Australia and around New
963 Zealand.

964

965 Marine air temperature shows widespread and significant warming, in agreement with HadNMAT2 (Kent et al.,
966 2013). Very few of the gridboxes with a negative trend are significant. In some cases they are in similar
967 locations to the drying trends seen in specific humidity and/or dew point temperature e.g., the coast south of
968 Australia around Tasmania, the east coast of Brazil. The warming is stronger in the northern mid-latitudes with
969 the Baltic, Mediterranean and Red Seas showing particularly strong warming consistent with strongly increasing
970 dew point temperature and specific humidity.

971

972 Whilst relative humidity is more sensitive to methodological choices and observational errors, the broad
973 spatially coherent structures to the regions of increasing and decreasing saturation, with broadscale significance,
974 are very encouraging in terms of data quality. Furthermore, the drying trends tend to be around the mid-latitudes
975 while the increasing saturation trends are more around the tropics, as seen over land. We still urge caution in the
976 use of marine relative humidity but these results collectively suggest that decreasing saturation might be a real
977 feature.

978

979 **5 Code and data availability**

980

981 HadISDH.marine is available as 5° by 5° gridded fields of monthly means and anomalies along with a 1981-
982 2010 climatology and uncertainty estimates at the gridbox scale. The data begin in January 1973 and continue to
983 December 2018 (at time of writing) and will be updated annually. HadISDH.marine is publicly available from
984 www.metoffice.gov.uk/hadobs/hadisdh/ under an Open Government license
985 (<http://www.nationalarchives.gov.uk/doc/open-government-licence/version/3/>) as netCDF and text files.
986 Processing code (Python) can also be made available on request. HadISDH.marine data, derived diagnostics and
987 plots can be found at www.metoffice.gov.uk/hadobs/hadisdh/indexMARINE.html and
988 <http://dx.doi.org/10.5285/463b2fcd6a264a39b1e3249dab16c177> (Willett et al., 2020). It should be cited using
989 this paper and the following: [Willett, K.M.; Dunn, R.J.H.; Kennedy, J.J.; Berry, D.I. \(2020\): HadISDH marine:
990 gridded global monthly ocean surface humidity data version 1.0.0.2018f. Centre for Environmental Data
991 Analysis, 5th August 2020. doi:10.5285/463b2fcd6a264a39b1e3249dab16c177.
992 <http://dx.doi.org/10.5285/463b2fcd6a264a39b1e3249dab16c177>. Willett, K. M., Dunn, R. J. H., Kennedy, J. J.
993 and Berry, D. I.: HadISDH.marine: gridded global monthly marine surface humidity data \(version 1.0.0.2018f\)
994 \[Data set\]. Met Office Hadley Centre HadOBS Datasets, , 2020.](#)

995
996 This product forms one of the HadOBS (www.metoffice.gov.uk/hadobs) climate monitoring products and will
997 be blended with the HadISDH.land product to create a global land and marine humidity monitoring product.
998 Updates and exploratory analyses are documented at <http://hadisdh.blogspot.co.uk> and through the Met Office
999 HadOBS twitter account @metofficeHadOBS.

1000

1001 **6 Discussion and conclusions**

1002

1003 Marine humidity data are susceptible to a considerable number of biases and sources of error that can be large in
1004 magnitude. We have cleaned the data where possible by applying quality control for outliers, supersaturation,
1005 repeated values and neighbour inconsistency which has removed up to 25 % of our initial selection in some
1006 years. We have also applied adjustments to account for biases arising from un-aspirated instrument types and
1007 differing observation heights over space and time. Care has also been taken to avoid diurnal and seasonal
1008 sampling biases as far as possible when building the gridded fields and the use of gridbox mean climate
1009 anomalies reduces remaining random error through averaging.

1010

1011 Spatial coverage of HadISDH.marine differs year to year. The coverage is generally poorer than seen for
1012 variables such as SST which benefit significantly from drifting buoy observations. Any further decline in
1013 observation and transmission of humidity from ships is of concern to our ability to robustly monitor surface
1014 humidity over oceans. Future versions may be able to make more use of humidity data from buoys but their
1015 proximity to the sea surface and difficulty of regular maintenance can lead to poor quality observations. The
1016 provision of digital metadata significantly improves our ability to quantify and account for biases in the data.
1017 Hence, the continuity of this metadata beyond 2014, and ideally an increase in quantity, also strongly affects our
1018 ability to robustly monitor ocean surface humidity. Given the current availability of ship data and metadata, and
1019 necessarily strict selection criteria and quality control, the resulting spatial coverage is good over the Northern
1020 Hemisphere outside of the high latitudes. There is very poor coverage over the Southern Hemisphere, especially
1021 south of 20° S. This means that our ‘global’ analyses are biased to the Northern Hemisphere. Care should be
1022 taken to account for different spatial coverage when comparing products. However, when comparing HadISDH
1023 to masked and unmasked ERA-Interim fields differences were surprisingly small.

1024

1025 We have shown that the observations are warm and moist relative to ERA-Interim reanalysis for the majority of
1026 the observed globe apart from the northwestern Pacific. This is despite ERA-Interim fields representing 2 m
1027 above the surface compared to the general observation heights of 10-30 m above the surface. Differences are
1028 largest around coastlines, particularly in the Red Sea and Persian Gulf. There is insufficient spatial coverage to
1029 produce a high resolution climatology from the data themselves, hence our use of ERA-Interim initially and then
1030 interpolated observation based fields. However, the lower resolution (5° by 5°) monthly mean climatologies
1031 from the final HadISDH.marine.1.0.0.2018f version show expected spatial patterns and have good spatial
1032 consistency, providing evidence that our data selection methods have resulted in reasonably high quality data.

1033

1034 The quality control and bias adjustment procedures have made small differences to the global average anomaly
1035 timeseries for specific humidity, dew point temperature and air temperature. This overall agreement in the
1036 global average timeseries between versions, and also between the daytime, night time and combined versions,
1037 increases confidence in the overall signal of increased moisture and warmth over oceans. These features show
1038 widespread spatial consistency in the HadISDH.marine.1.0.0.2018f gridbox decadal trends which also adds
1039 confidence. Hence, we can conclude that the ICOADS data are a useful source of humidity data for climate
1040 monitoring. However, we expect differences to be larger on smaller spatial scale analyses. HadISDH.marine

1041 shows consistency with other products in terms of long-term linear trends in the global averages. There are some
1042 differences year to year, with ERA-Interim showing warmer and moister anomalies prior to the early 1990s, and
1043 hence, smaller trends overall.

1044

1045 For relative humidity, differences between the versions can be large for any one year but the overall decreasing
1046 saturation trend appears to be robust. We conclude this because the trend is consistent across all processing
1047 steps, apparent in ERA-Interim fields and also has spatial consistency across the extratropics and mid-latitudes.
1048 This is a somewhat surprising result and one that should be treated cautiously. Theoretical and model-based
1049 analysis of changes in relative humidity over ocean under a warming climate suggest negligible or small
1050 positive changes (Held and Soden, 2006; Schneider et al., 2010; Byrne and O’Gorman, 2013, 2016, 2018). The
1051 temporal patterns in global average relative humidity are quite different to those over land whereas specific
1052 humidity shows similarity with the HadISDH.land timeseries, largely driven by the El Niño related peaks. The
1053 pre-1982 data have previously been noted as having a moist bias and our processing steps do not appear to have
1054 removed this feature. The trend excluding this earlier period (1982-2018) is no longer a significant decreasing
1055 trend and therefore more consistent with expectation. Removal of whole number flagged data appeared to
1056 exacerbate the pre-1982 bias and make the negative trends larger. Further work to assess the physical
1057 mechanisms that might lead to such trends is needed.

1058

1059 There are known issues with ERA-Interim in terms of its stability. For example, sea surface temperatures cooled
1060 around mid-2001 due to a change in the SST analysis product used (Simmons et al., 2014). This is very likely to
1061 affect humidity over the ocean surface in ERA-Interim. Similarly, changes in satellite streams over time can also
1062 affect the long-term stability of ERA-Interim, even in the surface fields. Also, the assimilated ship data are not
1063 adjusted for biases in the ERA-Interim assimilation. Clearly, there are various issues affecting both in-situ based
1064 monitoring products and reanalysis products such that neither one can be easily identified as the more accurate
1065 estimate. Analyses should take into account all available estimates and their strengths and weaknesses.

1066 Comparison of HadISDH.marine with satellite-based estimates of humidity over ocean will be an important next
1067 step.

1068

1069 We have attempted to quantify uncertainty in HadISDH.marine. The uncertainty analysis comprises observation
1070 uncertainty at the point of measurement which is then propagated through to gridbox averages taking correlation

1071 in space and time into account where relevant. Sampling uncertainty at the gridbox level due to uneven
1072 sampling across the gridbox in space and time is assessed. We have also provided uncertainty estimates in
1073 regional and global averages including coverage uncertainty. The propagation of gridbox observation and
1074 sampling uncertainty to large scale averages does not explicitly take into account correlation in these uncertainty
1075 quantities in space and time. As this is a first version monitoring product this simple method is seen as an
1076 appropriate first attempt to assess uncertainty. The ranges presented should be seen as a lower limit on the
1077 uncertainty. Overall, uncertainty in the global average is dominated by the coverage uncertainty for all variables
1078 except relative humidity and dew point depression. The total observation uncertainty is larger at the beginning,
1079 and especially the end of the record, where digital metadata are fewer or non-existent (post-2014). Overall, the
1080 uncertainty is small relative to the magnitude of long-term trends with the exception of relative humidity. We
1081 suspect that this is an overestimate at the gridbox level owing to assumptions of complete correlation in the
1082 height adjustment, instrument adjustment and climatology uncertainty components, and an underestimate at the
1083 regional average level given assumptions of no correlation. This is a first attempt to comprehensively quantify
1084 marine humidity uncertainty and future methodological improvements are envisaged.

1085

1086 We conclude that this first version marine humidity monitoring product is a reasonable estimate of large-scale
1087 trends and variability and contributes to our understanding of climate changes as a new and methodologically-
1088 independent analysis. The trends and variability shown are mostly in concert with expectation; widespread
1089 moistening and warming is observed over the oceans (excluding the mostly data-free Southern Hemisphere)
1090 from 1973 to present. These are also large relative to the magnitude of our uncertainty estimates. Our key
1091 finding is that the marine relative humidity appears to be decreasing (the air is becoming less saturated). We
1092 have explored various processes for ensuring high quality data and shown that these do not make large
1093 differences for large scale analyses of specific humidity, dew point temperature and air temperature but that
1094 there is greater sensitivity to methodological choices for relative humidity.

1095

1096 The spatial coverage of surface humidity data is very low outside of the Northern Hemisphere. If only those data
1097 with digitised metadata are included then this coverage deteriorates further. Although moored buoy numbers
1098 have increased dramatically since the 1990s, their measurements are more prone to error through proximity to
1099 the water, and hence, contamination, in addition to less frequent manual checking and maintenance. Hence, our

1100 ability to monitor surface humidity with any degree of confidence depends on the continued availability of ship
1101 data and provision of digitised metadata.

1102
1103 **Author Contributions**

1104
1105 Kate Willett undertook the majority of the methodology, coding, writing and plotting. John Kennedy designed
1106 and coded the quality control methodology and software with some contribution from Kate Willett. Robert
1107 Dunn designed and coded the gridding methodology and software with some contribution from Kate Willett.
1108 David Berry designed and reviewed the height adjustment methodology and provided guidance on marine
1109 humidity data biases, inhomogeneities and issues. All authors have contributed text and edits to the main paper.
1110

1111 **Competing Interests**

1112
1113 The authors declare that they have no conflict of interest.

1114
1115 **Acknowledgements**

1116
1117 Kate Willett, Robert Dunn and John Kennedy were supported by the Met Office Hadley Centre Climate
1118 Programme funded by BEIS and Defra. (GA01101).

1119
1120 **References**

1121
1122 Berry, D., 2009: Surface forcing of the North Atlantic: accuracy and variability, University of Southampton,
1123 176pp.

1124 Berry, D. I., Kent, E. C. and Taylor, P. K. : An analytical model of heating errors in marine air temperatures
1125 from ships, *J. Atmospheric and Oceanic Technology*, 21(8), 1198–1215, 2004.

1126
1127 Berry, D. I. and Kent, E. C. : A new air-sea interaction gridded dataset from ICOADS with uncertainty
1128 estimates, *Bulletin of the American Meteorological Society*, 90, 645-656, 2009.

1129
1130 Berry, D. I. and Kent, E. C.: Air–Sea fluxes from ICOADS: the construction of a new gridded dataset with
1131 uncertainty estimates, *Int. J. Climatol.*, 31, 987–1001, 2011.

1132
1133 BIPM, 2008: Evaluation of measurement data – Guide to the expression of uncertainty in measurement. JCGM
1134 100:2008. <https://www.bipm.org/en/publications/guides/gum.html>

1135
1136 Bojinski, S., M. Verstraete, T.C. Peterson, C. Richter, A. Simmons, and M. Zemp, 2014: [The Concept of](#)
1137 [Essential Climate Variables in Support of Climate Research, Applications, and Policy](#). *Bull. Amer. Meteor.*
1138 *Soc.*, 95, 1431–1443, <https://doi.org/10.1175/BAMS-D-13-00047.1>

1139
1140 Bosilovich, M. G., Akella, S., Coy, L., Cullather, R., Draper, C., Gelaro, R., Kovach, R., Liu, Q., Molod, A.,
1141 Norris, P., Wargan, K., Chao, W., Reichle, R., Takacs, L., Vikhliav, Y., Bloom, S., Collou, A., Firth, S.,
1142 Labow, G., Partyka, G., Pawson, S., Reale, O., Schubert, S. D. and Suarez, M. : MERRA-2: Initial Evaluation of
1143 the Climate, Technical Report Series on Global Modeling and Data Assimilation, Volume 43, NASA/TM–2015-
1144 104606/Vol. 43, pp. 136. <http://gmao.gsfc.nasa.gov/reanalysis/MERRA-2/docs/>, 2015.

1145
1146 Buck, A. L. : New equations for computing vapor pressure and enhancement factor, *J. Appl. Meteor.*, 20, 1527–
1147 1532, 1981.

1148
1149 Byrne, M. P. and P. A. O’Gorman, 2013: Link between land-ocean warming contrast and surface relative
1150 humidities in simulations with coupled climate models. *Geophysical Research Letters*, 40 (19), 5223-5227,
1151 <https://doi.org/10.1002/grl.50971>.

1152
1153 Byrne, M. P. and P. A. O’Gorman, 2016: Understanding decreases in land relative humidity with global
1154 warming: conceptual model and GCM simulations. *Journal of Climate*, 29, 9045-9061, DOI: 10.1175/JCLI-D-
1155 16-0351.1.

1156
1157 Byrne, M. P. and O’Gorman, P. A.: Trends in continental temperature and humidity directly linked to ocean
1158 warming, *Proceedings of the National Academy of Sciences USA*. 115(19), 4863-4868. doi:
1159 10.1073/pnas.1722312115, 2018.
1160
1161 Copernicus Climate Change Service (C3S) (2017): ERA5: Fifth generation of ECMWF atmospheric reanalyses
1162 of the global climate. Copernicus Climate Change Service Climate Data Store (CDS), February 2019.
1163 <https://cds.climate.copernicus.eu/cdsapp#!home>
1164
1165 Dai, A. : Recent climatology, variability, and trends in global surface humidity, *J. Climate.*, 19, 3589–3606,
1166 2006.
1167
1168 Dee, D. P., Uppala, S. M., Simmons, A. J., Berrisford, P., Poli, P., Kobayashi, S., Andrae, U., Balmaseda, M.
1169 A., Balsamo, G., Bauer, P., Bechtold, P., Beljaars, A. C. M., van de Berg, L. J., Bidlot, L., Bormann, N., Delsol,
1170 C., Dragani, R., Fuentes, M., Geer, A. J., Haimberger, L., Healy, S. B., Hersbach, H., Holm, E. V., Isaksen, L.,
1171 Kallberg, P., Kohler, M., Matricardi, M., McNally, A. P., Monge-Sanz, B. M., Morcrette, J.-J., Park, B.-K.,
1172 Peubey, C., de Rosnay, P., Tavolato, C., Thepaut, J.-N., and Vitart, F.: The ERA-Interim reanalysis:
1173 configuration and performance of the data assimilation system, *Q. J. Roy. Meteorol. Soc.*, 137, 553–597,
1174 doi:10.1002/qj.828, 2011.
1175 ~~Ebita, A., and co authors. : The Japanese 55 year reanalysis “JRA-55”: An interim report. SOLA, 7, 149–152,~~
1176 ~~doi:10.2151/sola.2011-038, 2011.~~
1177
1178 Elliott, W. P., Ross, R. J. and Schwartz, B. : Effects on climate records of changes in National Weather Service
1179 humidity processing procedures, *Journal of Climate*, 11, 2424-2436, 1998.
1180
1181 Freeman, E., Woodruff, S. D., Worley, S. J., Lubker, S. J., Kent, E. C., Angel, W. E., Berry, D. I., Brohan, P.,
1182 Eastman, R., Gates, L., Gloeden, W., Ji, Zaihua, Lawrimor, J., Rayner, N. A., Rosenhagen, G., Smith, S. R., :
1183 ICOADS Release 3.0: a major update to the historical marine climate record, *International Journal of*
1184 *Climatology*, 37 (5). 2211-2232.10.1002/joc.4775, 2017.
1185
1186 Gelaro, R., McCarty, W., Suárez, M. J., Todling, R., Molod, A., Takacs, L., Randles, C. A., Darmenov, A.,
1187 Bosilovich, M. G., Reichle, R., Wargan, K., Coy, L., Cullather, R., Draper, C., Akella, S., Buchard, V., Conaty,
1188 A., da Silva, A. M., Gu, W., Kim, G., Koster, R., Lucchesi, R., Merkova, D., Nielsen, J. E., Partyka, G.,
1189 Pawson, S., Putman, W., Rienecker, M., Schubert, S. D., Sienkiewicz, M. and Zhao, B., : The Modern-Era
1190 Retrospective Analysis for Research and Applications, Version 2 (MERRA-2). *J. Climate*, 30, 5419–
1191 5454,<https://doi.org/10.1175/JCLI-D-16-0758.1>, 2017.
1192
1193 Gilhousen, D., : A Field evaluation of NDBC Moored Buoy Winds, *Journal of Atmospheric and Oceanic*
1194 *Technology*, 4, 94 – 104, 1987.
1195
1196 Hartmann, D. L., Klein Tank, A. M. G., Rusticucci, M., Alexander, L. V., Brönnimann, S., Charabi, Y.,
1197 Dentener, F. J., Dlugokencky, E. J., Easterling, D. R., Kaplan, A., Soden, B. J., Thorne, P. W., Wild, M. and
1198 Zhai, P. M.: Observations: Atmosphere and Surface. In: *Climate Change 2013: The Physical Science Basis.*
1199 *Contribution of Working Group I to the Fifth Assessment Report of the Intergovernmental Panel on Climate*
1200 *Change* [Stocker, T. F., D. Qin, G.-K. Plattner, M. Tignor, S.K. Allen, J. Boschung, A. Nauels, Y. Xia, V. Bex
1201 and P.M. Midgley (eds.)]. Cambridge University Press, Cambridge, United Kingdom and New York, NY, USA,
1202 pp. 159 – 254, doi:10.1017/CBO9781107415324.008, 2013.
1203
1204 Held, I. M. and Soden, B. J., : Robust responses of the hydrological cycle to global warming. *Journal of*
1205 *Climate*, 19, 5686-5699, 2006.
1206
1207 Hersbach, H., de Rosnay, P., Bell, B., Schepers, D., Simmons, A., Soci, C., Abdalla, S., Alonso Balmaseda, M.,
1208 Balsamo, G., Bechtold, P., Berrisford, P., Bidlot, J., de Boissésón, E., Bonavita, M., Browne, P., Buizza, R.,
1209 Dahlgren, P., Dee, D., Dragani, R., Diamantakis, M., Flemming, J., Forbes, R., Geer, A., Haiden, T., Hólm, E.,
1210 Haimberger, L., Hogan, R., Horányi, A., Janisková, M., Laloyaux, P., Lopez, P., Muñoz-Sabater, J., Peubey, C.,
1211 Radu, R., Richardson, D., Thépaut, J.-N., Vitart, F., Yang, X., Zsótér, E. and Zuo, H.: Operational global
1212 reanalysis: progress, future directions and synergies with NWP, ERA Report 27, 63pp. Available from
1213 www.ecmwf.int, 2018.
1214

1215 Jensen, M. E., Burman, R. D. and Allen, R. G.: Evapotranspiration and Irrigation Water Requirements: A
1216 Manual. American Society of Civil Engineers, 332 pp, 1990
1217

1218 Jones, P. D., Osborn, T. J., and Briffa, K. R. : Estimating sampling errors in large-scale temperature averages,
1219 Journal of Climate, 10, 2548-2568, 1997.
1220

1221 Josey, S. A., Kent, E. C. and Taylor, P. K.: New insights into the ocean heat budget closure problem from
1222 analysis of the SOC air–sea flux climatology, J. Climate, 12, 2685–2718, 1999.
1223

1224 Kennedy, J. J., Rayner, N. A., Smith, R. O., Saunby, M. and Parker, D. E. : Reassessing biases and other
1225 uncertainties in sea-surface temperature observations since 1850 part 1: measurement and sampling errors, J.
1226 Geophys. Res., 116, D14103, doi:10.1029/2010JD015218, 2011a.
1227

1228 Kennedy, J. J., Rayner, N. A., Smith, R. O., Saunby, M. and Parker, D. E. : Reassessing biases and other
1229 uncertainties in sea-surface temperature observations since 1850 part 2: biases and homogenisation, J. Geophys.
1230 Res., 116, D14104, doi:10.1029/2010JD015220, 2011b.
1231

1232 Kennedy, J. J., Rayner, N. A., Atkinson, C. P., & Killick, R. E. : An ensemble data set of sea-surface
1233 temperature change from 1850: the Met Office Hadley Centre HadSST.4.0.0.0 data set, Journal of Geophysical
1234 Research: Atmospheres, 124. <https://doi.org/10.1029/2018JD029867>, 2019.
1235

1236 Kent, E. C. and Challenor, P. G. : Towards estimating climatic trends in SST. Part II: random errors, Journal of
1237 Atmospheric and Oceanic Technology. 23, 476-486. DOI: 10.1175/JTECH1844.1, 2006.
1238

1239 Kent, E. C., and Taylor, P. K. : Accuracy of humidity measurement on ships: Consideration of solar radiation
1240 effects, J. Atmos. Oceanic Technol., 13, 1317–1321, 1996.
1241

1242 Kent, E. C., Tiddy, R. J. and Taylor, P. K.: Correction of marine air temperature observations for solar radiation
1243 effects, J. Atmos. Oceanic Technol., 10, 900–906, 1993.
1244

1245 Kent, E. C., Woodruff, S. D. and Berry D. I. : Metadata from WMO Publication No. 47 and an Assessment of
1246 Voluntary Observing Ship Observation Heights in ICOADS, J. Atmospheric and Oceanic Technology 2007
1247 24:2, 214-234, doi: <http://dx.doi.org/10.1175/JTECH1949.1>, 2007.
1248

1249 Kent, E. C., Rayner, N. A., Berry, D. I., Saunby, M., Moat, B. I., Kennedy, J. J. and Parker, D. E. : Global
1250 analysis of night marine air temperature and its uncertainty since 1880: The HadNMAT2 data set, J. Geophys.
1251 Res. Atmos., 118, doi:10.1002/jgrd.50152, 2013.
1252

1253 Kent, E. C., Berry, D. I., Prytherch, J., Roberts, J. B. : [A comparison of global marine surface-specific humidity
1254 datasets from *in situ* observations and atmospheric reanalysis](https://doi.org/10.1002/joc.3691), International Journal of Climatology, 34 (2). 355-
1255 376.<https://doi.org/10.1002/joc.3691>, 2014.
1256

1257 [Kobayashi, S., Ota, Y., Harada, Y., Ebata, A., Moriya, M., Onoda, H., Onogi, K., Kamahori, H., Kobayashi, C.,
1258 Endo, H., Miyaoka, K., and Takahashi, K.: The JRA-55 reanalysis: general specifications and basic
1259 characteristics. J. Meteor. Soc. Japan, 93, 5–48. <https://doi.org/10.2151/jmsj.2015-001>, 2015.](https://doi.org/10.2151/jmsj.2015-001)
1260

1261 [Menne, M. J. and Williams Jr., C. N. : Homogenization of Temperature Series via Pairwise Comparisons.
1262 Journal of Climate, 22, 1700-1717. DOI: 10.1175/2008JCLI2263.1](https://doi.org/10.1175/2008JCLI2263.1)
1263 [Met Office Hadley Centre; National Oceanography Centre, 2019: HadISDH.marine: gridded global monthly
1264 marine surface humidity data version 1.0.0.2018f. Centre for Environmental Data Analysis, *date of citation*:
1265 ~~doi:xx.xxxx/XXXXX~~–\(FINALISED-AFTER-REVIEW\)](https://www.metoffice.gov.uk/hadobs/hadisdh)
1266

1267 Peixoto, J. P., and Oort, A. H. : The climatology of relative humidity in the atmosphere, J. Climate, 9, 3443–
1268 3463, 1996.
1269

1270 Rayner, N. A., Parker, D. E., Horton, E. B., Folland, C. K., Alexander, L. V., Rowell, D. P., Kent, E. C., Kaplan,
1271 A. : Global analyses of sea surface temperature, sea ice, and night marine air temperature since the late
1272 nineteenth century, Journal of Geophysical Research – Atmospheres, 108, No. D14, 4407.
1273 <https://doi.org/10.1029/2002JD002670>, 2003.
1274

1275 Rayner, N., Brohan, P., Parker, D., Folland, C., Kennedy, J., Vanicek, M., Ansell, T. and Tett, S. : Improved
1276 analyses of changes and uncertainties in sea surface temperature measured in situ since the mid-nineteenth
1277 century: The HadSST2 data set, *J. Clim.*, 19(3), 446–469, doi:10.1175/JCLI3637.1, 2006.
1278

1279 Santer, B. D., Thorne, P. W., Haimberger, L., Taylor, K. E., Wigley, T. M. L., Lanzante, J. R., Solomon, S.,
1280 Free, M., Gleckler, P. J., Jones, P. D., Karl, T. R., Klein, S. A., Mears, C., Nychka, D., Schmidt, G. A.,
1281 Sherwood, S. C. and Wentz, F. J.: Consistency of modelled and observed temperature trends in the tropical
1282 troposphere. *Int. J. Climatol.*, 28, 1703-1722. doi:[10.1002/joc.1756](https://doi.org/10.1002/joc.1756), 2008.
1283 Schneider, T., O 'Gorman, P. A. and Levine, X. J.,: Water vapor and the dynamics of climate changes, *Reviews*
1284 *in Geophysics*, 48, RG3001, doi:10.1029/2009RG000302, 2010.
1285

1286 Simmons, A., Willett, K. M., Jones, P. D., Thorne, P. W., and Dee, D.: Low-frequency variations in surface
1287 atmospheric humidity, temperature and precipitation: inferences from reanalyses and monthly gridded
1288 observational datasets, *J. Geophys. Res.*, 115, D01110, doi:10.1029/2009JD012442, 2010.
1289

1290 Simmons, A. J., Poli, P., Dee, D. P., Berrisford, P., Hersbach, H., Kobayashi S. and Peubey, C. : Estimating
1291 low-frequency variability and trends in atmospheric temperature using ERA-Interim, *Q.J.R. Meteorol. Soc.*,
1292 140: 329-353. doi:[10.1002/qj.2317](https://doi.org/10.1002/qj.2317), 2014.
1293

1294 Smith, S. D.: Wind stress and heat flux over the ocean in gale force winds. *J. Physical Oceanography*, 10, 709-
1295 726, 1980.

1296 Smith, S. D. : Coefficients for sea surface wind stress, heat flux and wind profiles as a function of wind speed
1297 and temperature, *J. Geophys. Res.*, 93, 15467-15472, 1988.

1298 Stull, R. B. : *An Introduction to Boundary Layer Meteorology* Kluwer Academic Publishers, 666 pp, 1988.

1299 Wade, C. G.,: An evaluation of problems affecting the measurement of low relative humidity on the United
1300 States radiosonde, *Journal of Atmospheric and Oceanic Technology*, 11, 687-700, 1994.

1301 Willett, K. M., Jones, P. D., Gillett N. P. and Thorne, P. W.: Recent changes in surface humidity: development
1302 of the HadCRUH dataset, *J. Climate*, 21, 5364–5383, 2008.
1303

1304 Willett, K. M., Williams Jr., C. N., Dunn, R. J. H., Thorne, P. W., Bell, S., de Podesta, M., Jones, P. D. and
1305 Parker, D. E. : HadISDH: An updated land surface specific humidity product for climate monitoring. *Climate of*
1306 *the Past*, 9, 657-677, doi:10.5194/cp-9-657-2013, 2013.
1307

1308 Willett, K. M., Dunn, R. J. H., Thorne, P. W., Bell, S., de Podesta, M., Jones, P. D., Parker, D. E. and Williams
1309 Jr., C. N.: HadISDH land surface multi-variable humidity and temperature record for climate monitoring,
1310 *Climate of the Past*, 10, 1983-2006, doi:10.5194/cp-10-1983-2014, 2014.
1311

1312 ~~[Willett, K.M.; Dunn, R.J.H.; Kennedy, J.J.; Berry, D.I. \(2020\): HadISDH marine: gridded global monthly ocean](#)~~
1313 ~~[surface humidity data version 1.0.0.2018f. Centre for Environmental Data Analysis, 5th August 2020.](#)~~
1314 ~~[doi:10.5285/463b2fcd6a264a39b1e3249dab16c177.](https://doi.org/10.5285/463b2fcd6a264a39b1e3249dab16c177)~~
1315 ~~[http://dx.doi.org/10.5285/463b2fcd6a264a39b1e3249dab16c177.](http://dx.doi.org/10.5285/463b2fcd6a264a39b1e3249dab16c177)~~ ~~Willett, K. M., Dunn, R. J. H., Kennedy, J. J.~~
1316 ~~and Berry, D. I.: HadISDH marine: gridded global monthly marine surface humidity data (version 1.0.0.2018f)~~
1317 ~~[Data set]. Met Office Hadley Centre HadOBS Datasets, , 2020.~~
1318

1319 Willett, K. M., Berry, D., Bosilovich, M. and Simmons, A.: [Global Climate] Surface Humidity [in “State of the
1320 Climate in 2018”], *Bulletin of the American Meteorological Society*, accepted, 2019.

1321 Wolter, K.,: Trimming problems and remedies in COADS, *Journal of climate*. 10. 1980-1997. DOI:
1322 10.1175/1520-0442(1997)010<1980:TPARIC>2.0.CO;2, 1997.
1323

1324 Woodruff, S.,: Archival of data other than in IMMT format: The International Maritime Meteorological Archive
1325 (IMMA) format. NOAA Earth System Research Laboratory (ESRL), Boulder, CO, USA.
1326 <http://icoads.noaa.gov/e-doc/imma/R2.5-imma.pdf>, 2010.
1327
1328
1329
1330

1331
 1332
 1333
 1334
 1335
 1336
 1337
 1338
 1339
 1340
 1341
 1342
 1343
 1344
 1345
 1346
 1347
 1348
 1349
 1350
 1351
 1352
 1353
 1354
 1355
 1356
 1357
 1358
 1359
 1360
 1361
 1362
 1363
 1364
 1365
 1366
 1367
 1368
 1369
 1370
 1371
 1372
 1373
 1374
 1375
 1376
 1377
 1378
 1379
 1380
 1381
 1382
 1383

Tables

Table 1. Description of quality control tests.

Test	Description	1st and 2nd Iteration	3rd Iteration and Bias Adjusted	% of Observations Removed
day / night	values likely to be affected by the solar heating of a ship where the sun was above the horizon an hour before the observation (based on the month, day, hour, latitude and	flagged	flagged	NA

	longitude; Kent et al. (2013)) are flagged as 'day'			
climatology	T and T_d must be within a specified threshold of the nearest 1° by 1° pentad climatology	removed	removed	$T = 2.39$ and $T_d = 5.14$
supersaturation	T_d must not be greater than T (only T_d removed)	removed	removed	0.54
track	The distance and direction travelled by the ship must be plausible and consistent with the time between observations, normal ship speeds and observation locations before and after.	removed	removed	0.86
repeated value	A T or T_d value must not appear in more than 70 % of a ship track where there are at least 20 observations.	removed	removed	$T = 0.04$ and $T_d = 0.06$
repeated saturation	Saturation ($T_d = T$) must not persist for more than 48 hours within a ship track where there are at least 4 observations (only T_d removed).	removed	removed	0.54
buddy	T and T_d must be within a specified threshold of the average of nearest neighbours in space and time.	not applied	removed	$T = 7.16$ and $T_d = 9.47$
whole number	A T or T_d value must not appear as a whole number in more than 50 % of a ship track where there are at least 20 observations.	flagged	flagged	$T = 11.73$ and $T_d = 8.20$

1384
1385
1386
1387
1388
1389
1390
1391
1392
1393
1394
1395
1396
1397
1398
1399
1400
1401
1402
1403
1404
1405
1406
1407
1408
1409
1410
1411

Table 2. Description of the uncertainty elements affecting marine humidity. All uncertainties are assessed as 1σ uncertainty.

Uncertainty Source		Description	Type	Formula	Correlation
U_i	Non-aspirated instrument adjustment uncertainty. Expressed as q (g kg^{-1}) and then propagated to	Adjusted poorly aspirated instrument: 0.2 g kg^{-1} in terms of q (following Berry and Kent, 2011	standard	0.2	Space and time, $r = 1$

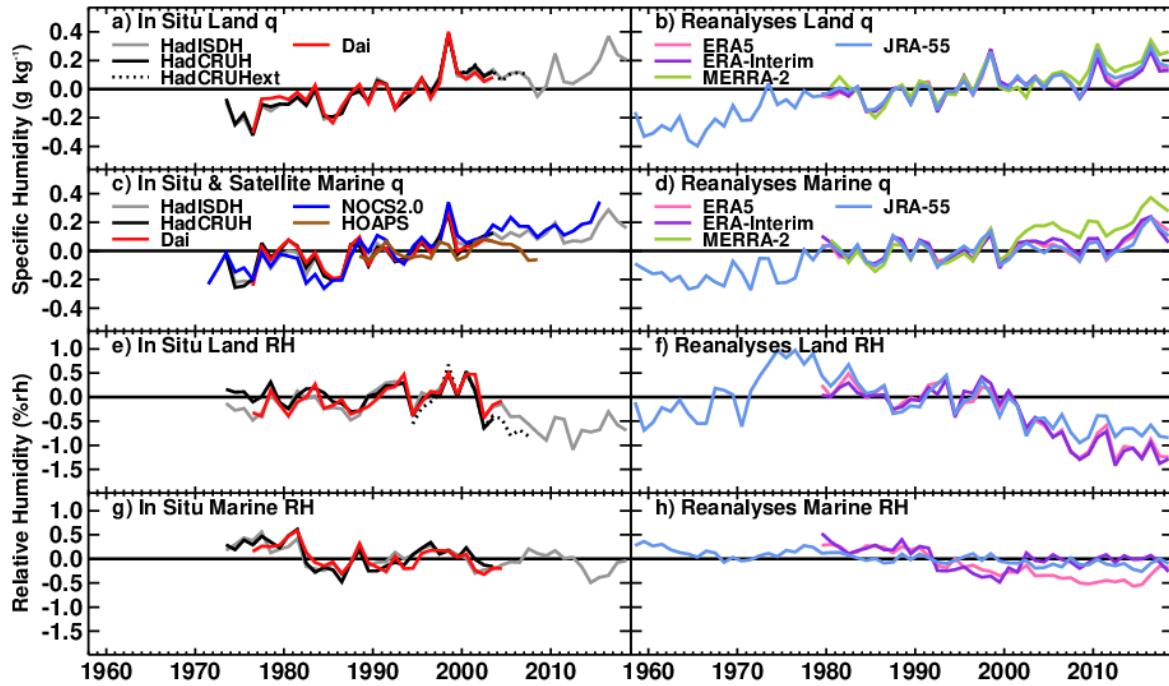
	other humidity variables	standard uncertainty assessment).			
		Partially adjusted unknown instrument: 0.2 g kg ⁻¹ + the full adjustment amount in terms of q .			
				$0.2 + 100 \left(\frac{abs(q - q_{adj})}{55} \right)$	
U_h	Observation height adjustment uncertainty. Expressed as T (°C) and q (g kg ⁻¹) and then propagated to other humidity variables	Height adjusted ship and valid SST: assessed using the range of adjustments from a 1σ uncertainty in the height estimate.	normally distributed	$\frac{xH_{max} - xH_{min}}{2}$	Space and time, $r = 1$
		Height adjusted ship and invalid SST or height adjusted buoy: the larger of the adjustment value or 0.1 °C in terms of T and $0.007q$.	normally distributed	x_{adj} Or 0.1 °C in terms of T $0.007q_{adj}$	
		Height adjustment or uncertainty range not resolved, valid SST: half of the difference between the observation value and the surface value (SST or q_{sf}).	standard	$\frac{T_{(adj)} - SST}{2}$ $\frac{q_{(adj)} - q_{sf}}{2}$ $q_{sf} = 0.98q_{sat}f(SST)$	
		Height adjustment or uncertainty range not resolved, no valid SST: 0.1 °C in terms of T and $0.007q$.	standard	0.1 °C in terms of T $0.007q_{adj}$	
U_m	Measurement uncertainty. Expressed as T (°C), T_w (°C) and RH (%rh) and then propagated to other humidity variables.	Standard uncertainty in the thermometer (T) and psychrometer (T_w) is 0.2 °C and 0.15 °C respectively.	standard	0.2 °C in terms of T 0.15 °C in terms of T_w x %rh depending on the temperature and RH bins in Table S3	None, $r = 0$

		This equates in an uncertainty in RH dependent on T .			
U_w	Whole number uncertainty. Expressed as T (°C) and T_d (°C) and then propagated to other humidity variables.	Observation either has the Whole Number flag set or is a whole number and from a red listed source deck in Table S4.	uniformly distributed	$\frac{0.5}{\sqrt{3}}$	None, $r = 0$
		If both T and T_d are offending whole numbers then RH, T_w and DPD have a combined uncertainty.		$\frac{1}{\sqrt{3}}$	
U_c	Climatology uncertainty. Assessed for each variable independently.	The 1° by 1° pentad gridbox climatological standard deviation for the variable is divided by the square root of the number of observations used to create it.	standard	$\frac{\sigma_{clim}}{\sqrt{N_{obs}}}$	Space and time, $r = 1$
U_{og}	Total observation uncertainty of the gridbox	All gridbox observation uncertainty sources are combined, assuming no correlation between sources.	standard	$\sqrt{U_i^2 + U_h^2 + U_m^2 + U_w^2 + U_c^2}$	Space and time to some extent, decreasing with space and time
U_{sg}	Temporal and spatial sampling uncertainty of the gridbox	Sampling uncertainty follows Jones et al., (1997) depending on the mean 'station' variance, the mean inter-site correlation and the number of 'stations' contributing to the gridbox.	standard	$\frac{(\bar{s}_i^2 \bar{r}(1 - \bar{r}))}{(1 + (N_s - 1)\bar{r})}$	Space and time to some extent, decreasing with space and time

U_{fg}	Full uncertainty of the gridbox	All gridbox uncertainty sources are combined, assuming no correlation between sources.	standard	$\sqrt{U_{og}^2 + U_{sg}^2}$	Space and time to some extent, decreasing with space and time
----------	---------------------------------	--	----------	------------------------------	---

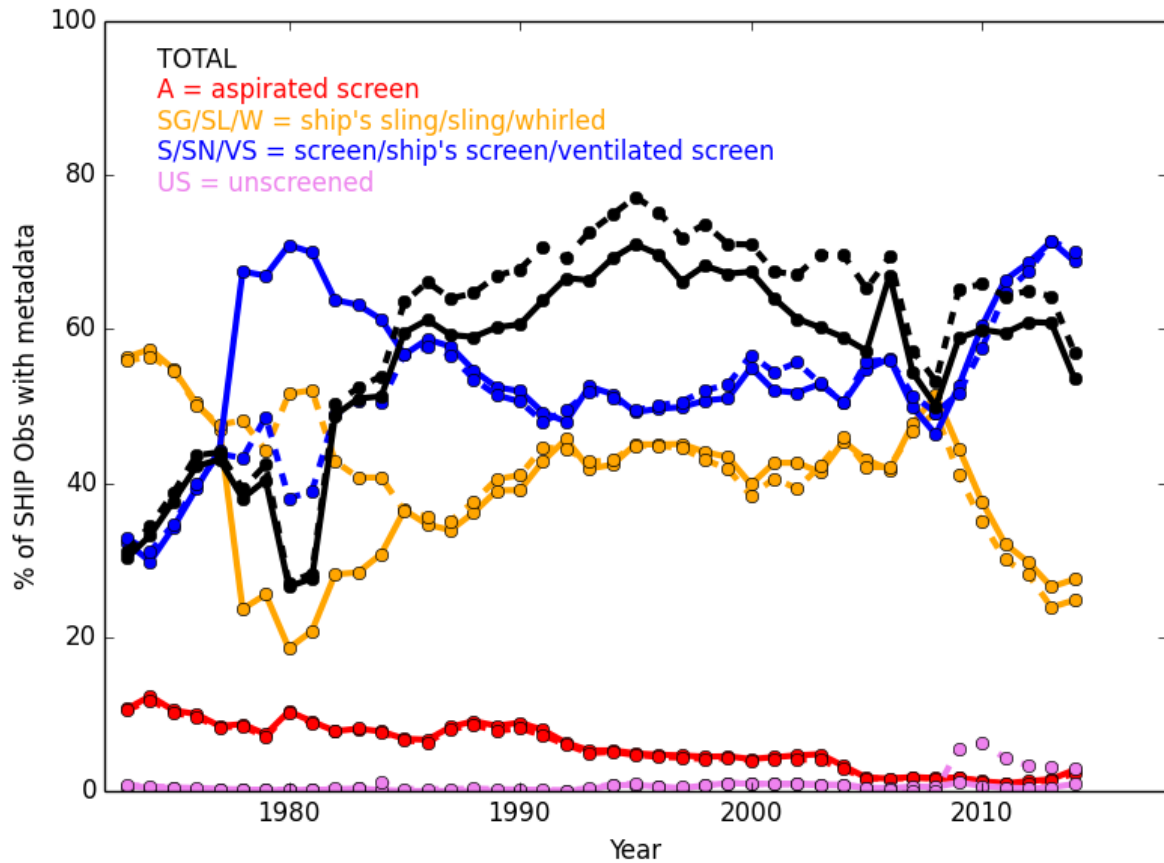
1412
1413
1414
1415
1416
1417
1418
1419
1420
1421
1422
1423
1424
1425
1426
1427
1428
1429
1430
1431
1432
1433
1434
1435
1436
1437
1438
1439
1440
1441
1442
1443
1444
1445
1446
1447
1448
1449
1450
1451
1452
1453
1454

Figures



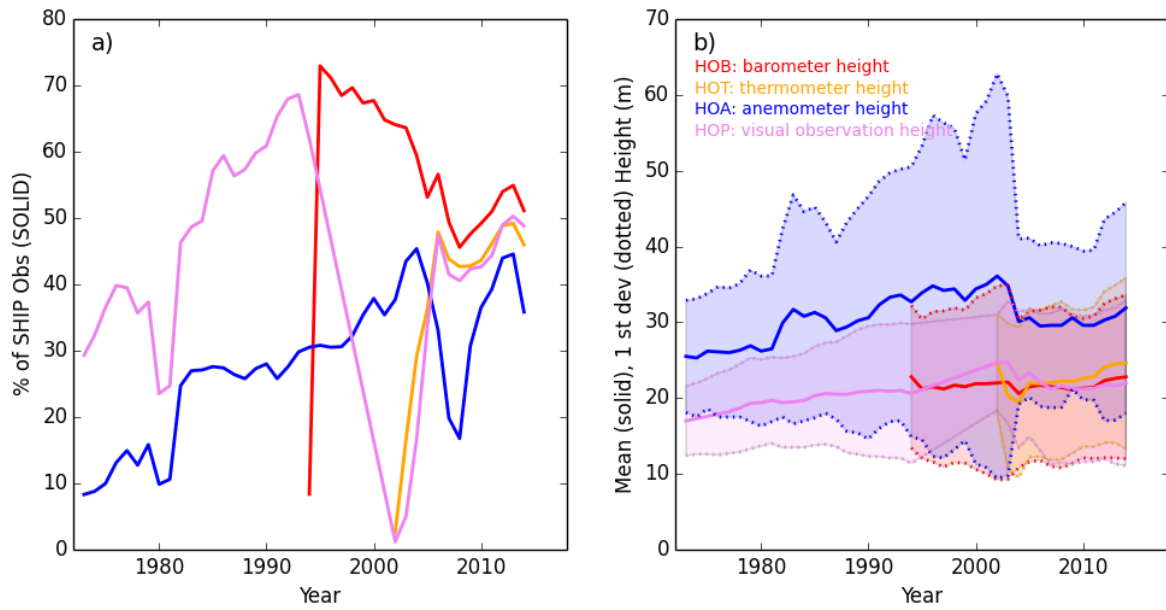
1455
 1456
 1457
 1458
 1459
 1460
 1461
 1462
 1463
 1464
 1465
 1466
 1467

Figure 1 Global average surface humidity annual anomalies (base period: 1979–2003). For in-situ datasets, 2-m surface humidity is used over land and ~10-m over the oceans. For the reanalysis, 2-m humidity is used across the globe. For ERA-Interim and ERA5, ocean-only points over open sea are selected and background forecast values are used as opposed to analysis values to avoid incorporating biases from unadjusted ship data. All data have been given a mean of zero over the common period 1979–2003 to allow direct comparison, with HOAPS given a zero mean over the 1988–2003 period. [Sources: HadISDH (Willett et al., 2013, 2014); HadCRUH (Willett et al., 2008); Dai (Dai 2006); HadCRUHext (Simmons et al. 2010); NOCSv2.0 (Berry and Kent, 2009, 2011); HOAPS (Fennig et al. 2012), ERA-Interim (Dee et al., 2011), ERA5 (C3S 2017, Hersbach et al., 2018), MERRA-2 (Gelaro et al. 2017; Bosilovich et al. 2015) and JRA-55 (KobayashiEbita et al. 2015)]. Adapted from Willett et al., 2019.

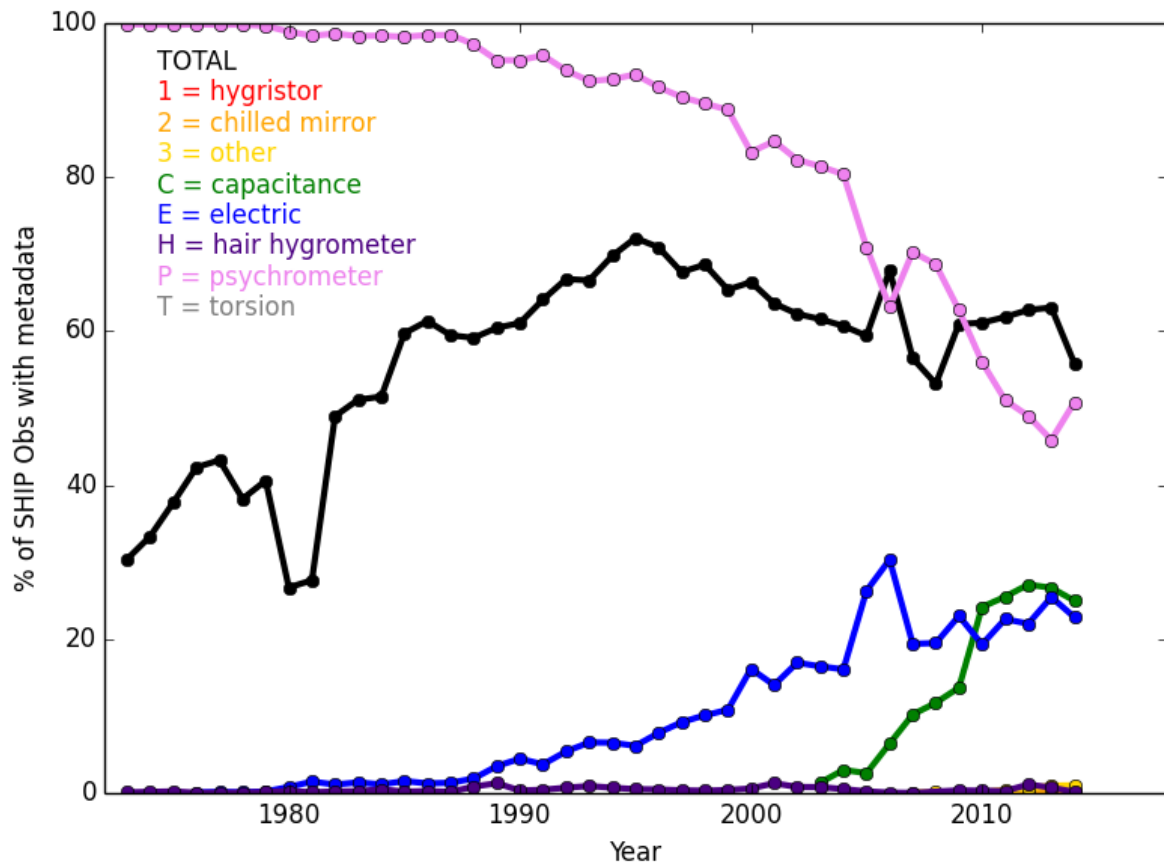


1468
 1469
 1470
 1471
 1472
 1473
 1474
 1475
 1476
 1477
 1478
 1479
 1480

Figure 2 Availability of instrument exposure information (black) for ships (platform (PT) = 0, 1, 2, 3, 4, 5) for the hygrometer (EOH, SOLID) and thermometer (EOT, DASHED) for each year. All ICOADS 3.0.0/3.0.1 observations passing 3rd iteration quality control are included. The percentage of EOHs/EOTs in each exposure category is also shown. Aspirated (A) screens are shown in red. Handheld instruments (ship's sling [SG], sling [SL], whirling [W]) are shown in orange. Unaspirated/unventilated screens (S) and ship's screens (SN) are shown in blue. Additionally, ventilated screens (VS) are also shown in blue as these are generally not artificially aspirated. Unscreened (US observations are shown in violet.



1481 Figure 3 a) Availability of instrument height information for ships (platform (PT) = 0, 1, 2, 3, 4, 5) for the
 1482 barometer (HOB), thermometer (HOT), anemometer (HOA) and visual observing platform (HOP) with b) mean
 1483 heights (solid lines) and standard deviations (dotted lines) for each year. All ICOADS 3.0.0/3.0.1 observations
 1484 passing 3rd iteration quality control are included.
 1485
 1486
 1487
 1488
 1489
 1490
 1491
 1492
 1493
 1494
 1495
 1496
 1497
 1498
 1499
 1500
 1501
 1502
 1503
 1504
 1505
 1506
 1507
 1508
 1509
 1510
 1511
 1512
 1513
 1514
 1515
 1516



1517
 1518 Figure 4 Availability of instrument type information (black) for ships (platform (PT) = 0, 1, 2, 3, 4, 5) for the
 1519 hygrometer (TOH) for each year. All ICOADS 3.0.0/3.0.1 observations passing 3rd iteration quality control are
 1520 included. The percentage of TOHs in each type category is also shown.
 1521
 1522
 1523
 1524
 1525
 1526
 1527
 1528
 1529
 1530
 1531
 1532
 1533
 1534
 1535
 1536
 1537
 1538
 1539
 1540
 1541
 1542
 1543
 1544
 1545
 1546
 1547
 1548

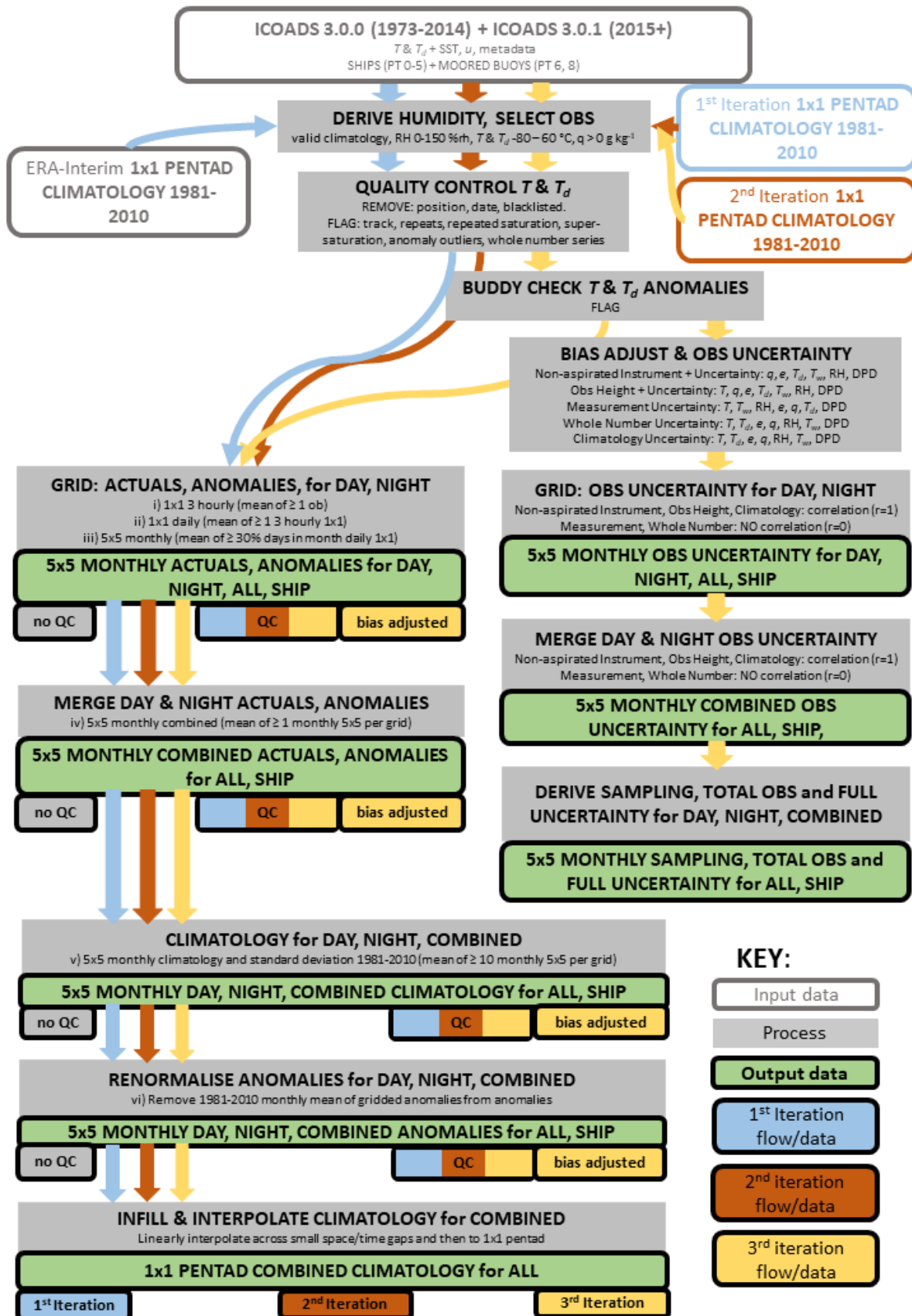
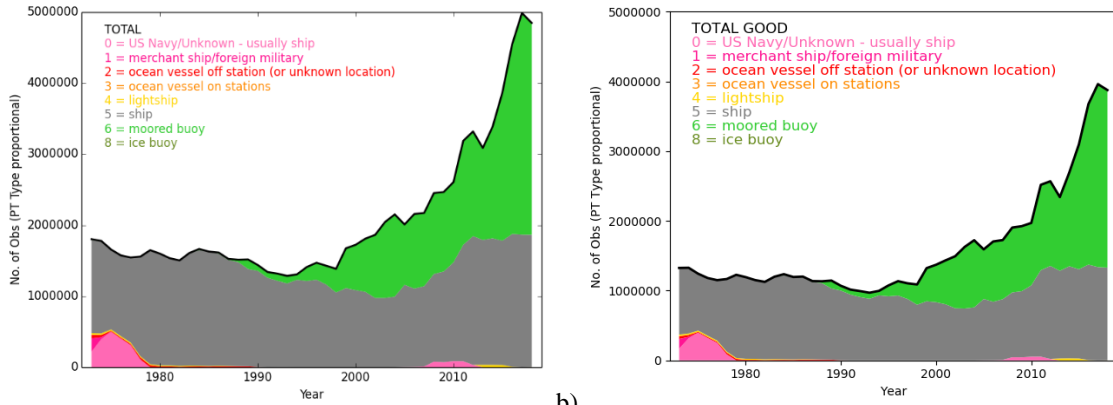


Figure 5 Flow chart of the build process from raw hourly observations to gridded fields. Note that the greyblue 'no QC' output boxes are produced during the 1st iteration by selecting all data rather than those passing quality control.

1554



1555

a)

1556

Figure 6 Annual observation count for the initial selection (a) and only those observations passing the final 3rd iteration quality control (b), broken down by platform (PT) type.

1557

1558

1559

1560

1561

1562

1563

1564

1565

1566

1567

1568

1569

1570

1571

1572

1573

1574

1575

1576

1577

1578

1579

1580

1581

1582

1583

1584

1585

1586

1587

1588

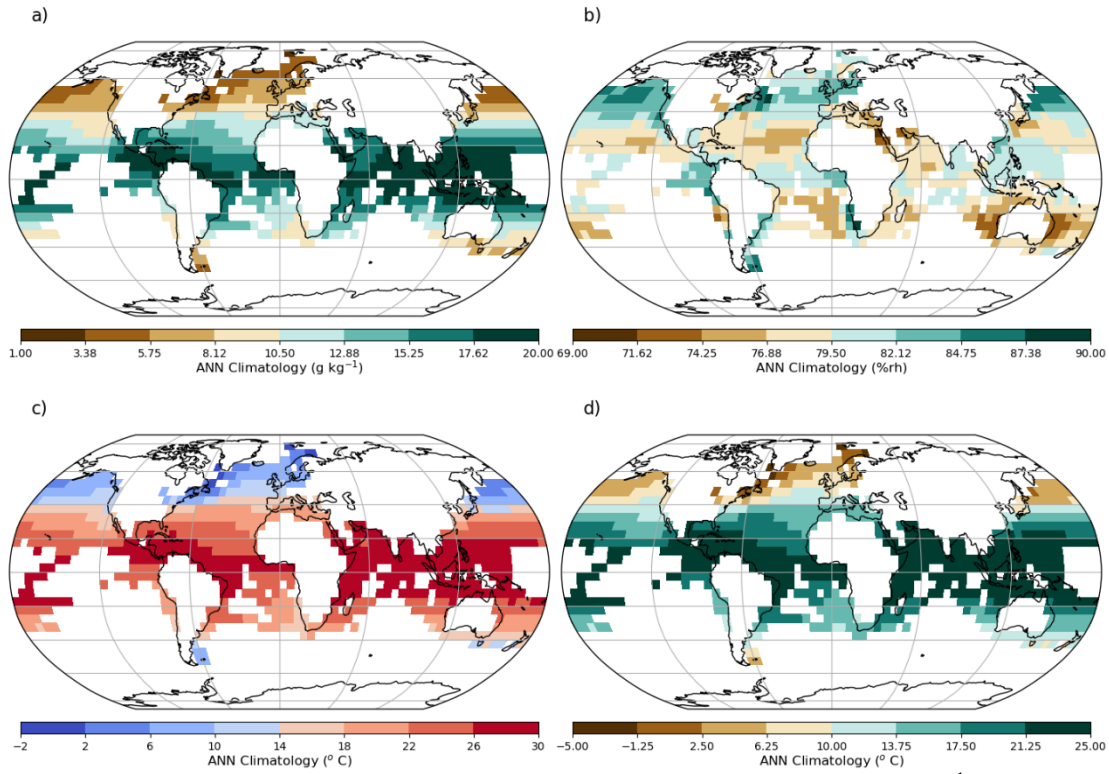
1589

1590

1591

1592

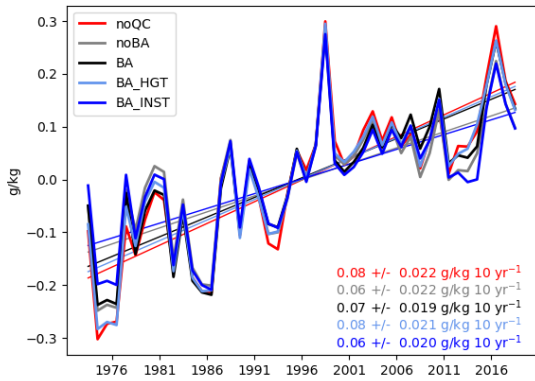
1593



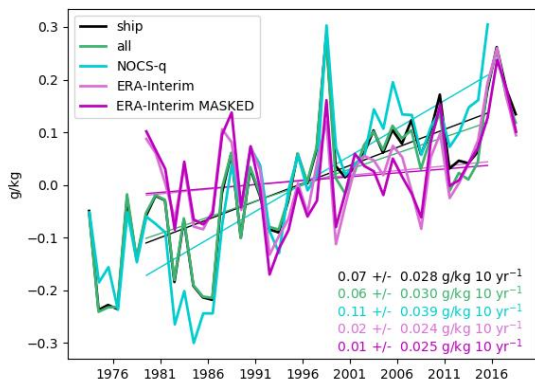
1594

1595
 1596
 1597
 1598
 1599
 1600
 1601
 1602
 1603
 1604
 1605
 1606
 1607
 1608
 1609
 1610
 1611
 1612
 1613
 1614
 1615
 1616
 1617

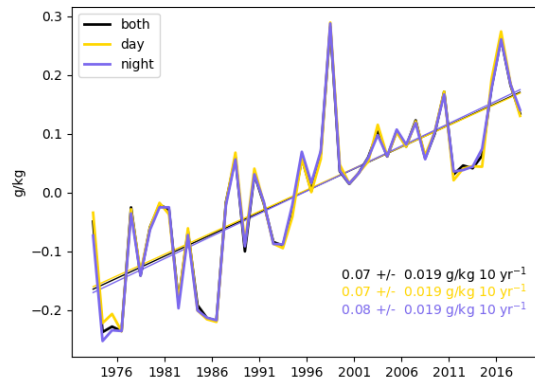
Figure 7 Annual mean climatologies relative to 1981-2010 for a) specific humidity (g kg^{-1}), b) relative humidity (%rh), c) air temperature ($^{\circ}\text{C}$) and d) dew point temperature ($^{\circ}\text{C}$) for 3rd iteration quality-controlled and bias-adjusted ship version. Climatological means are calculated for gridboxes and months with at least 10 years present over the climatology period. Annual mean climatologies require at least 9 months of the year to be represented climatologically.



1618 a)

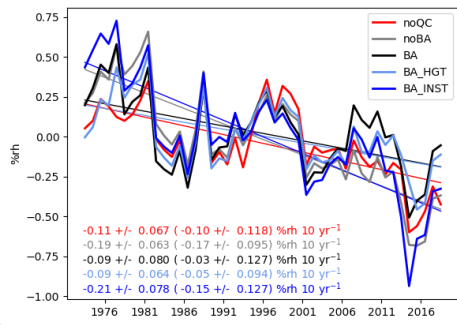


1619 b)

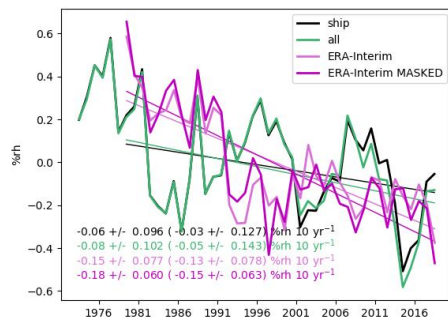


1620 c)

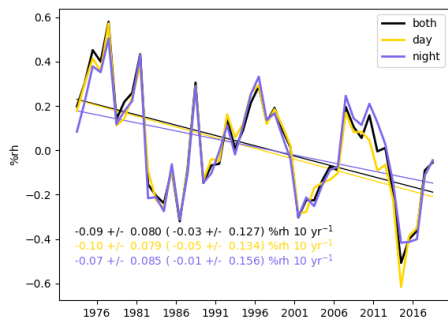
1621 Figure 8 Global annual average anomaly timeseries and decadal trends (\pm 90 % confidence interval) for
 1622 specific humidity. a) Processing comparison for ships only: raw data (noQC), 3rd iteration quality-controlled
 1623 with no bias adjustment (noBA), 3rd iteration quality-controlled and bias-adjusted (BA), 3rd iteration quality-
 1624 controlled and bias-adjusted for ship height only (BA_HGT), 3rd iteration quality-controlled and bias-adjusted
 1625 for instrument ventilation only (BA_INST). b) Platform and alternative product comparison: 3rd iteration
 1626 quality-controlled and bias-adjusted ship-only (ship), 3rd iteration quality-controlled and bias-adjusted for ships
 1627 and moored buoys (all), NOCSv2.0 in-situ quality-controlled and bias-adjusted product based on ships only
 1628 (NOCS-q), ERA-Interim reanalysis 2m fields using complete ocean coverage at the 1° by 1° scale (ERA-
 1629 Interim), ERA-Interim reanalyses 2m fields using complete ocean coverage at the 1° by 1° scale and masked to
 1630 HadISDH.marine spatio-temporal coverage (ERA-Interim MASKED). Trends cover the common 1979 to 2015
 1631 period. 1979 to 2018 trends for ERA-Interim are 0.03 ± 0.028 and 0.03 ± 0.027 for the full and masked versions
 1632 respectively. c) Time of observation comparison for 3rd iteration quality-controlled and bias-adjusted ship-only:
 1633 all times (both), daytime hours only (day), night time hours only (night). Linear trends were fitted using
 1634 ordinary least squares regression with AR(1) correction applied when calculating confidence intervals (Santer et
 1635 al., 2008).



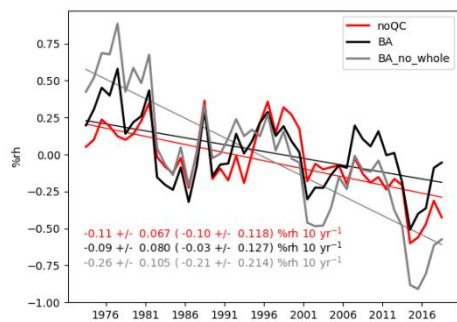
1636 a)



1637 b)

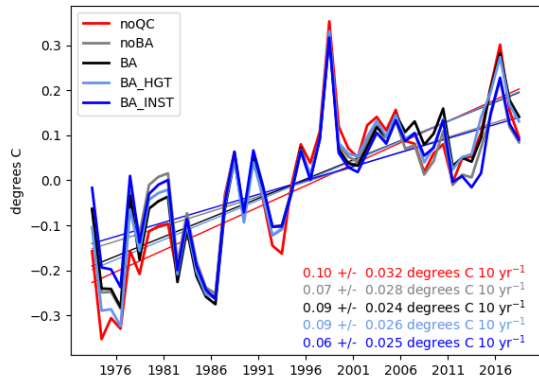


1638 c)

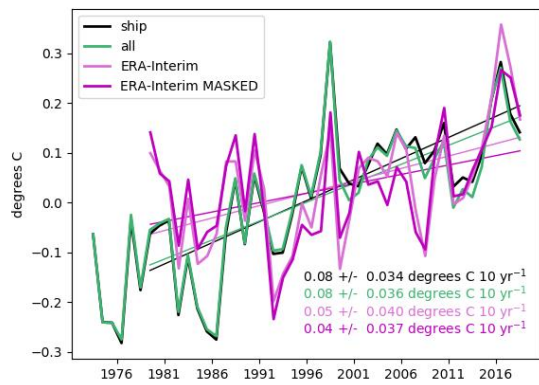


1639 d)

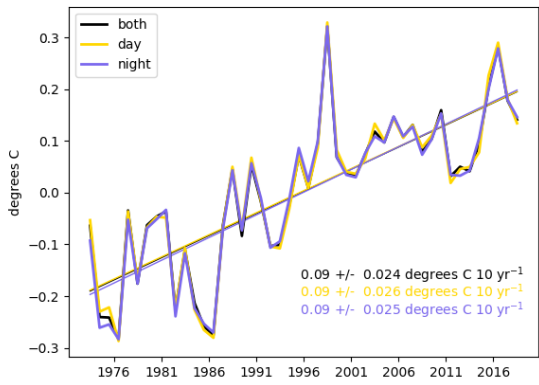
1640 Figure 9 Global annual average anomaly timeseries and decadal trends (\pm 90 % confidence interval) for
 1641 relative humidity. See Figure 8 caption for details. In addition, panel d) shows the timeseries from the bias
 1642 adjusted data with removal of any data with a whole number flag set (BA_no_whole). Trends in b) cover the
 1643 common 1979 to 2018 period and all trends in parentheses cover the 1982-2018 period.
 1644



1645 a)

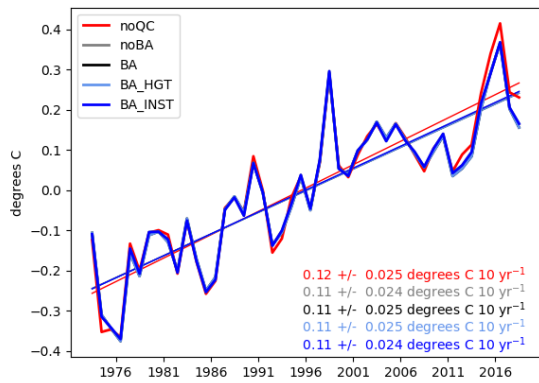


1646 b)

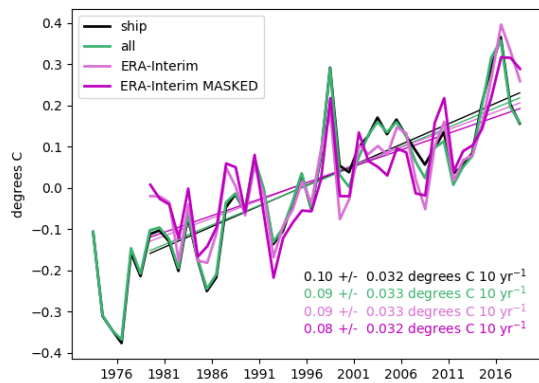


1647 c)

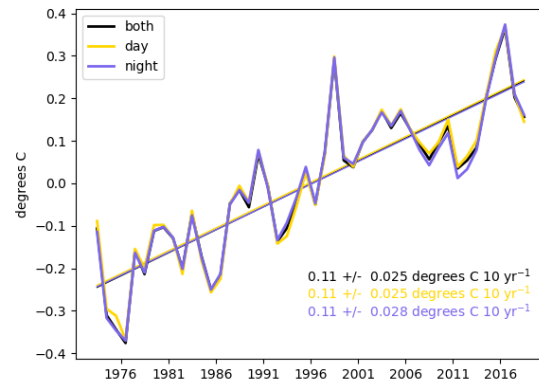
1648 Figure 10 Global annual average anomaly timeseries and decadal trends (\pm 90 % confidence interval) for dew
 1649 point temperature. See Figure 8 caption for details. Trends in b) cover the common 1979 to 2018 period.



1650 a)

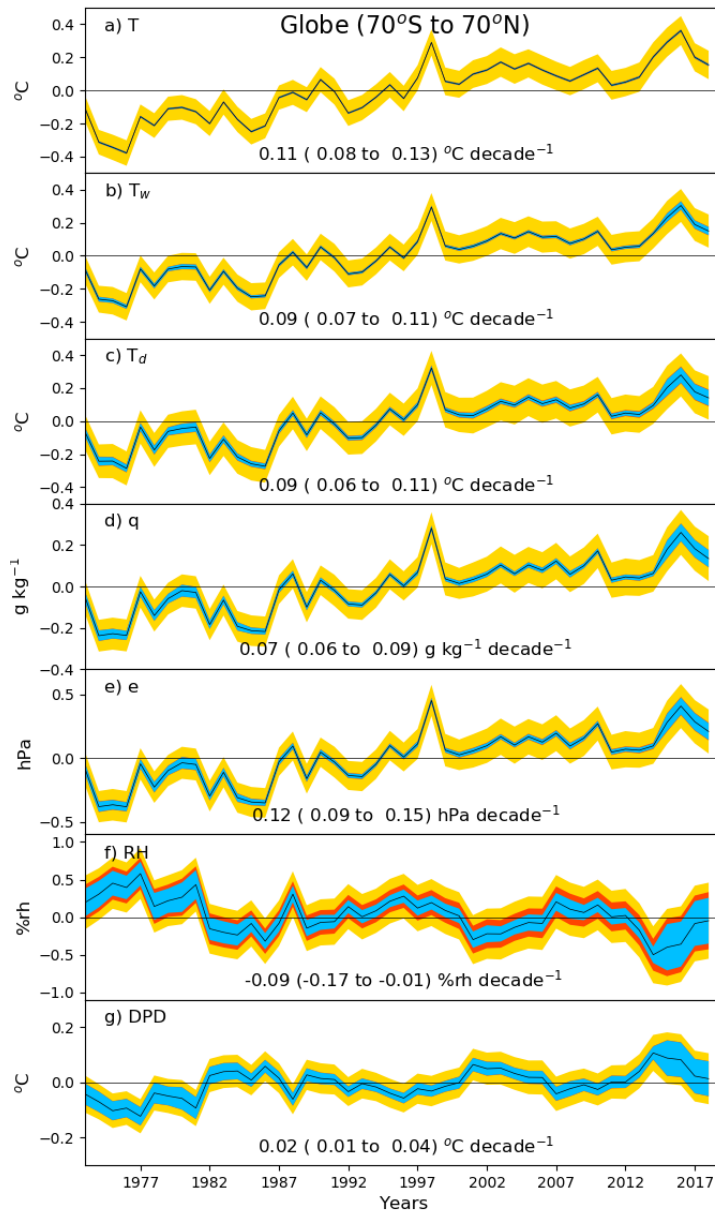


1651 b)



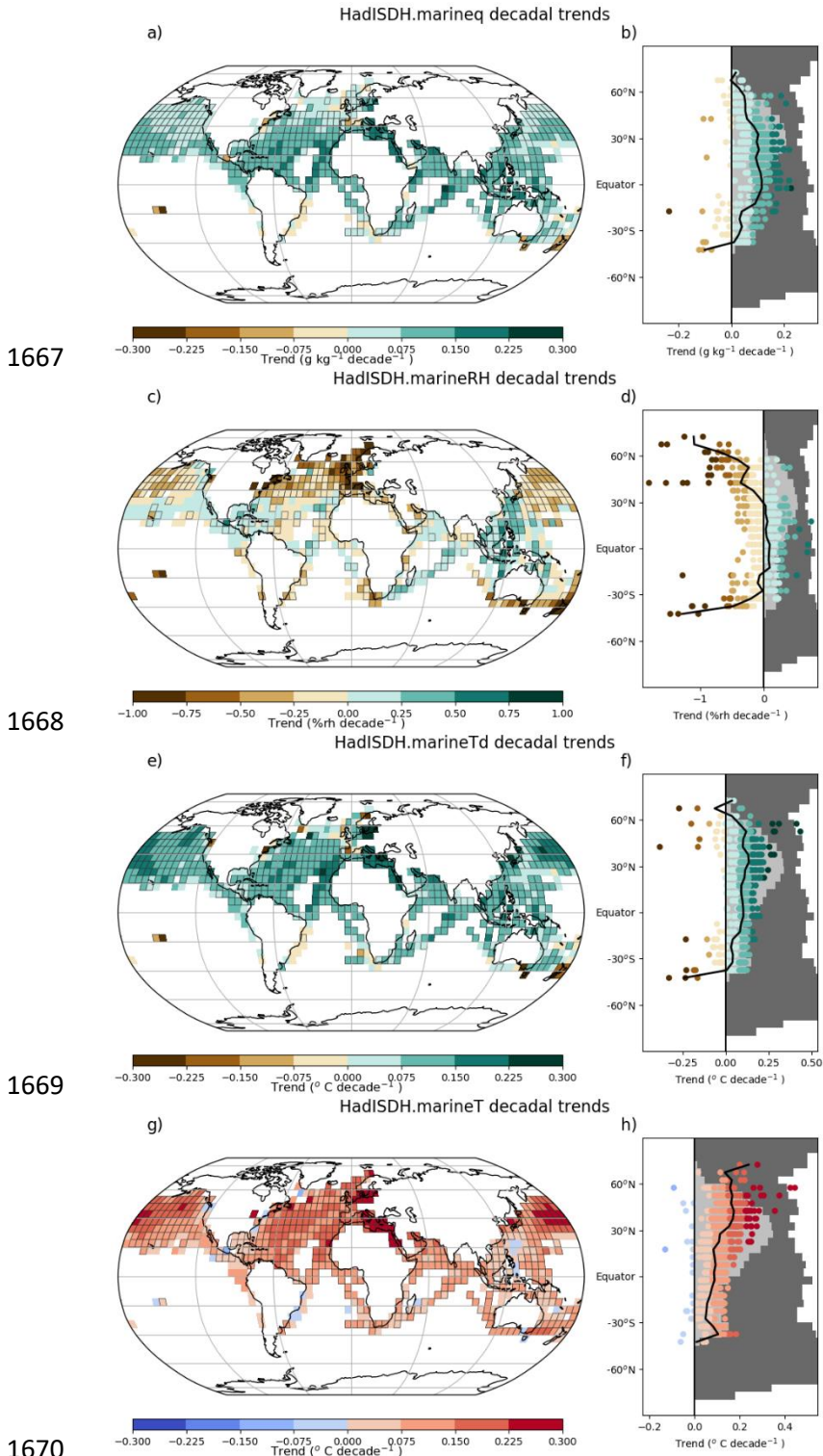
1652 c)

1653 Figure 11 Global annual average anomaly timeseries and decadal trends ($\pm 90\%$ confidence interval) for
 1654 marine air temperature. See Figure 8 caption for details. Trends in b) cover the common 1979 to 2018 period.
 1655



1656
 1657
 1658
 1659
 1660
 1661
 1662
 1663
 1664
 1665
 1666

Figure 12 Global average timeseries of annual mean climate anomalies for all variables. The 2 sigma uncertainty ranges for total observation (blue), sampling (red) and coverage (gold) uncertainty contributions combined are shown. All series have been given a zero mean over the common 1981-2010 period. Decadal linear trends and 90th percentile confidence intervals (in parentheses) were fitted using ordinary least squares regression with AR(1) correction applied when calculating the confidence intervals (Santer et al., 2008), with the range representing the 90 % confidence interval in the trend.



1667
1668
1669
1670
1671
1672
1673
1674
1675
1676
1677
1678
1679

Figure 13 Linear decadal trends from 1973 to 2018 for a, b) specific humidity (g kg^{-1}), c, d) relative humidity ($\%rh$), e, f) dew point temperature ($^{\circ}\text{C}$) and g, h) air temperature ($^{\circ}\text{C}$) for the 3rd iteration quality-controlled and bias-adjusted ships only. Decadal linear trends were fitted using ordinary least squares regression when there are at least 70 % percent of months present over the trend period. Gridboxes with boundaries show significant trends in that the 90 % confidence interval (calculated with AR(1) correction following Santer et al., 2008) around the trend magnitude is the same sign as the trend and does not encompass zero. The right-hand panels (b, d, f, h) show the distribution of gridbox trends by latitude with the mean shown as a solid black line. The dark grey shading shows the proportion of the globe at that latitude which is ocean. The light grey shading shows the proportion of the globe that contains observations.